One of the ER chaperones, the 150-kDa oxygen-regulated protein (ORP150), was originally identified in cultured astrocytes exposed to hypoxia [13]. Previous studies showed that expression of ORP150 is up-regulated under various pathological conditions and this up-regulation is implicated in the progression of these diseases [14,15].

It was recently suggested that IPF also involves the ER stress response, with GRP78 showing increased expression in the lungs of IPF patients and bleomycin-administered mice [16–18]. Genetic studies have revealed that mutations in the gene encoding surfactant protein C (SP-C, a protein produced by lung epithelial cells) could lead to familial interstitial pneumonia (a familial form of IPF) [19,20]. These mutations induce the ER stress response due to the accumulation of misfolded pro-SP-C [16,21]. However, because that induction of the ER stress response was observed in IPF patients without these mutations [16,18], the mechanism and role of ER stress response in IPF patients is unknown at present. Based on the cytoprotective effect provided by ER chaperones, it was considered that they would have a negative impact on the development of IPF (i.e. protective roles against IPF); however, no direct evidence (such as genetic evidence) exists to substantiate this. On the other hand, it was recently reported that the ER stress response stimulates the myofibroblastic differentiation of fibroblasts and EMT of lung epithelial cells *in vitro* [18,22]. Therefore, it is also possible that the ER stress response has a positive influence on the development of IPF. Thus, to understand the role of ER stress response in IPF, it may prove useful in the first instance to examine artificially induced pulmonary fibrosis in transgenic mice expressing each protein related to the response.

In line with this, we compare here aspects of bleomycin-induced pulmonary fibrosis in heterozygous ORP150-deficient mice ($ORP150^{+/-}$ mice) and wild-type mice. Bleomycin-induced pulmonary inflammatory responses were slightly exacerbated, while pulmonary fibrosis and dysfunction were clearly ameliorated in $ORP150^{+/-}$ mice compared to wild-type mice. We also found that bleomycin-induced increases in the pulmonary levels of both active TGF-β1 and myofibroblasts were suppressed in $ORP150^{+/-}$ mice. These results suggest that ORP150 is stimulative for bleomycin-induced pulmonary fibrosis, though at the same time ORP150 exerts a protective action against bleomycin-induced lung damage.

2. Materials and methods

2.1. Animals

Mice heterozygous for a truncated/inactivated mutant form of ORP150 ($ORP150^{+/-}$) and their wild-type counterparts ($ORP150^{+/+}$) (6–8 weeks of age) were prepared as described previously [12]. The experiments and procedures described here were carried out in accordance with the Guide for the Care and Use of Laboratory Animals as adopted and promulgated by the National Institutes of Health, and were approved by the Animal Care Committee of Keio University and Kumamoto University.

2.2. Administration of bleomycin, preparation of bronchoalveolar lavage fluid (BALF), assay for MPO activity, analysis of lung function and histological and immunohistochemical analyses

Mice were maintained under anaesthesia with chloral hydrate (500 mg/kg) and were given one intratracheal injection of bleomycin (5 mg/kg) to induce pulmonary fibrosis.

BALF was collected by cannulating the trachea and lavaging the lung with 1 ml of sterile PBS containing 50 units/ml heparin (two times). The total cell number in the BALF was counted using a haemocytometer. Cells were stained with Diff-Quik reagents and the ratios of alveolar macrophages, lymphocytes and neutrophils to total cells were determined. More than 200 cells were counted for each sample.

Myeloperoxidase (MPO) activity in the lung was measured as described previously [23].

Analysis of lung function was performed with a computer-controlled small-animal ventilator (FlexiVent; SCIREQ, Montreal, Canada) as described previously [24].

Histological and immunohistochemical analyses were done as described previously [24].

2.3. Hydroxyproline determination and ELISA for active TGF-β1

Hydroxyproline content was determined as described [25]. The active TGF-β1 content in the lung was determined by ELISA as described previously [24].

2.4. Immunoblotting analysis and real-time RT-PCR analysis

Total protein was prepared as described previously [26]. Samples were applied to polyacrylamide SDS gels and subjected to electrophoresis, after which the proteins were immunoblotted with an antibody against ORP150.

Real-time RT-PCR was performed as previously described [27]. The primers used were (name: forward primer, reverse primer): *Orp150*: 5′-gaagatgcagagcccatttc-3′, 5′-tctgctccaggacctcctaa-3′; *α-sma*: 5′-catcatgcgtctggatctgg-3′, 5′-ggacaatctcacgctcagca-3′; *E-cadherin*: 5′-tgcccagaaaatgaaaaagg-3′, 5′-gtgtatgtggcaatgcgttc-3′; *Col1a1*: 5′-ccctgtctgcttcctgtaaact-3′, 5′-catgttcggttggtcaaagata-3′; *actin*: 5′-ggacttcgagcaagagatgg-3′, 5′-agcactgtgttggcgtacag-3′.

2.5. Transfection

The siRNA for ORP150 was purchased from Qiagen. Cells were transfected with the siRNA using HiPerFect transfection reagents (Invitrogen) according to the manufacturer's instructions.

The plasmid for overexpression of ORP150 was constructed by insertion of the *Orp150* gene in pCI-neoORP150 [28] into pcDNA3.1 (Invitrogen). The transfection was carried out using Lipofectamine LTX (Invitrogen).

2.6. Statistical analysis

All values are expressed as the mean ± S.E.M. or S.D. Two-way analysis of variance followed by the Tukey test was used to evaluate differences between more than three groups. Differences were considered to be statistically significant for values of $p < 0.05$.

3. Results

3.1. Effect of down-regulation of ORP150 expression on bleomycin-induced pulmonary inflammatory responses

Pulmonary inflammation and fibrosis were induced by a once-only (at day 0) intratracheal administration of bleomycin, as described previously [25]. First, we monitored the expression of ORP150 in lung tissues by immunoblotting. As shown in Fig. 1A–D, treatment of mice with bleomycin increased the pulmonary level of ORP150 in $ORP150^{+/-}$ mice and wild-type mice, though the $ORP150^{+/-}$ mice showed lower ORP150 expression than the wild-type mice both in the presence and absence of bleomycin treatment.

The bleomycin-induced inflammatory response can be monitored in terms of the number of inflammatory cells in BALF after the administration of bleomycin [25]. As shown in Fig. 2A, the total

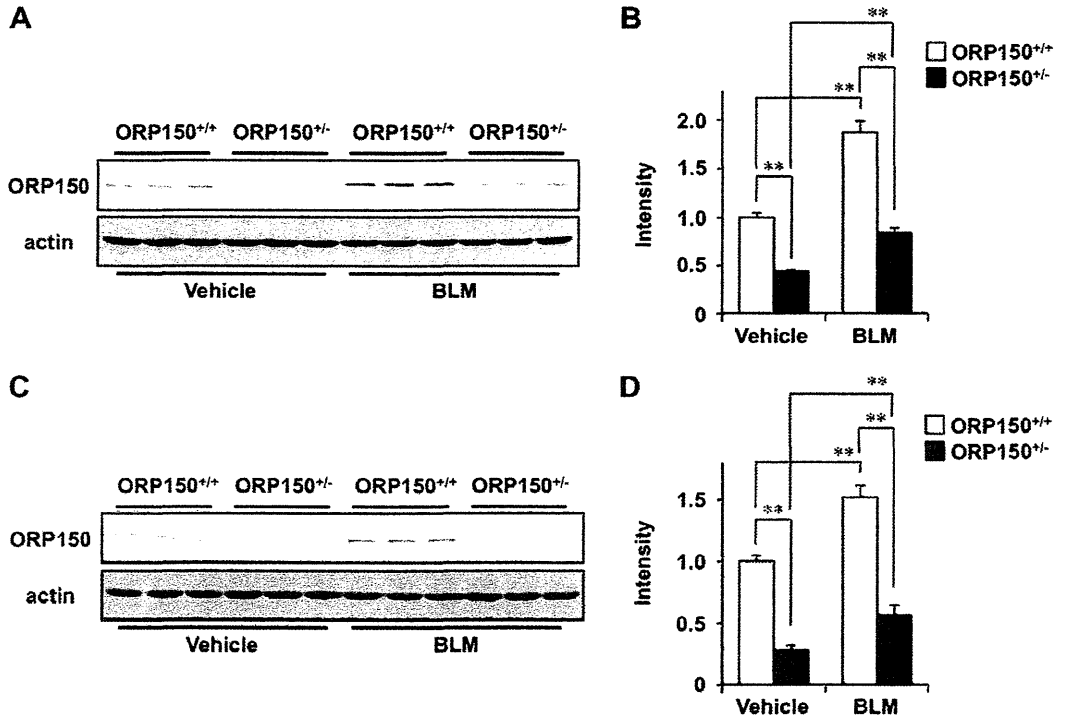

Fig. 1. Bleomycin-induced expression of ORP150 in the lung. ORP150$^{+/-}$ mice and wild-type mice (ORP150$^{+/+}$) were treated with (BLM) or without (Vehicle) bleomycin (5 mg/kg) once-only on day 0. Lungs were excised on day 3 (A and B) or 14 (C and D). Tissue homogenates were analysed by immunoblotting with antibodies against ORP150 or actin (A and C). The band intensity of ORP150 was determined and normalised to actin intensity (B and D). Values are mean ± S.E.M. ($n = 3$). $^{**}p < 0.01$. Scale bar, 50 μm.

number of inflammatory cells and individual numbers of alveolar macrophages, lymphocytes and neutrophils were all increased on day 3 after the bleomycin treatment. Compared to wild-type mice, this increase was slightly enhanced in ORP150$^{+/-}$ mice (Fig. 2A). Similar results were observed for MPO activity, an indicator of the inflammatory infiltration of leucocytes (Fig. 2B). These results suggest that ORP150 expression protects against bleomycin-induced inflammatory response.

3.2. Effect of down-regulation of ORP150 expression on bleomycin-induced pulmonary fibrosis, alteration of lung mechanics and respiratory dysfunction

Bleomycin-induced pulmonary fibrosis can be assessed by histopathological analysis and measurement of hydroxyproline levels. Haematoxylin and eosin (H & E) staining and Masson's trichrome staining of collagen revealed that bleomycin-induced collagen deposition was less apparent in ORP150$^{+/-}$ mice than in wild-type mice (Fig. 3A and B). Bleomycin also increased pulmonary hydroxyproline levels, although to a lesser degree in the ORP150$^{+/-}$ mice compared with wild-type mice (Fig. 3C). These results suggest that bleomycin-induced pulmonary fibrosis is less extensive in ORP150$^{+/-}$ mice compared to wild-type mice.

We then examined the effect of ORP150 expression on bleomycin-induced alterations of lung mechanics using a computer-controlled small-animal ventilator. Total respiratory system elastance (elastance of total lung including bronchi, bronchioles and alveoli) and tissue elastance (elastance of alveoli) were indistinguishable between heterozygous and wild-type mice in the absence of bleomycin treatment (Fig. 3D). In contrast, both types of mice showed increases in these parameters in response to bleomycin treatment, with this effect being more prominent in wild-type mice. These results suggest that the bleomycin-induced alteration of lung mechanics is ameliorated by the down-regulation of ORP150 expression.

As shown in Fig. 3E, FVC was indistinguishable between vehicle-treated ORP150$^{+/-}$ and wild-type mice, but was clearly decreased by the bleomycin treatment in wild-type mice while remaining unchanged in ORP150$^{+/-}$ mice (Fig. 3E). These results suggest that ORP150 expression exacerbates bleomycin-induced respiratory dysfunction.

To elucidate the mechanism underlying this stimulative effect of ORP150 on pulmonary fibrosis, we focused our attention on myofibroblast and TGF-β1. As shown in Fig. 4A, a bleomycin-dependent increase in the expression of α-SMA, a myofibroblast marker, was suppressed in ORP150$^{+/-}$ mice compared to wild-type mice, suggesting that the expression of ORP150 stimulates an increase in pulmonary myofibroblast number in the presence of bleomycin.

As shown in Fig. 4B, active TGF-β1 was increased by the bleomycin treatment; however the level was lower in ORP150$^{+/-}$ mice than in wild-type mice. These results suggest that ORP150 expression also stimulates a bleomycin-dependent increase in active TGF-β1 in lung tissue.

3.3. Effect of ORP150 expression on the TGF-β1-induced EMT of epithelial cells and differentiation of fibroblasts in vitro

As described in Section 1, an increase in pulmonary myofibroblasts associated with fibrosis is due to the stimulation of EMT of epithelial cells and the myofibroblastic differentiation of fibroblasts. We tested whether the expression of ORP150 affects these phenomena by examining *in vitro* the effect of siRNA for ORP150 on the TGF-β1-dependent alteration of expression of EMT-related genes in cultured human type II alveolar (A549) cells. Treatment of cells with TGF-β1 down-regulated the expression of the epithelial cell

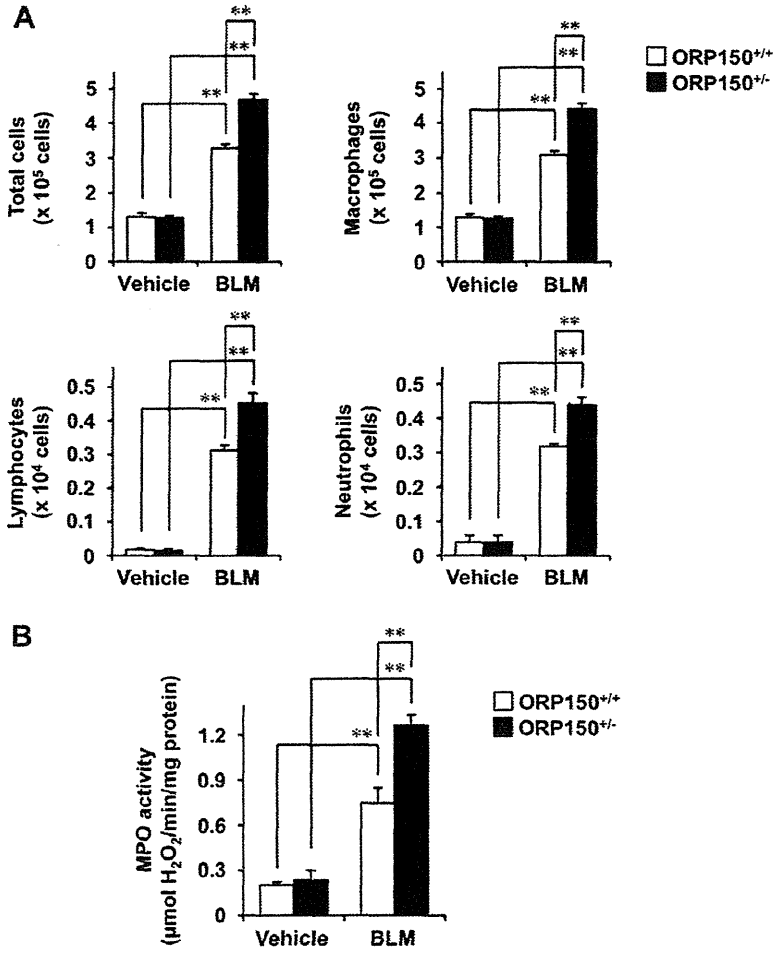

Fig. 2. Effect of down-regulation of ORP150 expression on bleomycin-induced pulmonary inflammatory responses. ORP150$^{+/-}$ mice and wild-type mice (ORP150$^{+/+}$) were treated with (BLM) or without (Vehicle) bleomycin (5 mg/kg) once-only on day 0 and lung tissue or BALF was obtained on day 3. Total cell number and individual numbers of alveolar macrophages, lymphocytes and neutrophils in BALF were counted (A). MPO activities in lung homogenates were determined (B). Values are mean ± S.E.M. $^{**}p < 0.01$.

marker *E-cadherin* mRNA (Fig. 4C), suggesting that TGF-β1 induces the EMT-like phenotype of A549 cells. Transfection of cells with siRNA for ORP150 suppressed the expression of *Orp150* mRNA but did not affect the expression of *E-cadherin* mRNA in the presence or absence of TGF-β1 (Fig. 4C). These results suggest that ORP150 expression does not affect the EMT of lung epithelial cells.

We also examined the effect of ORP150 expression on TGF-β1-dependent myofibroblastic differentiation of fibroblasts *in vitro*. Treatment of human embryonic lung fibroblasts (HFL-I cells) with TGF-β1 induced the expression of α-*sma* and *col1a1* mRNAs (Fig. 4D), suggesting that TGF-β1 activates the transition of fibroblasts to myofibroblasts. The transfection of cells with siRNA for ORP150 slightly decreased the expression of α-*sma* and *col1a1* mRNAs in the presence of TGF-β1 (Fig. 4D). We then examined the effect of overexpression of ORP150 on the myofibroblastic differentiation of fibroblasts. As shown in Fig. 4E, slightly increased the expression of α-*sma* and *col1a1* mRNAs was observed in the presence of TGF-β1. These results suggest that ORP150 expression stimulates the TGF-β1-dependent myofibroblastic differentiation of fibroblasts.

4. Discussion

Pulmonary fibrosis is triggered by pulmonary damage and inflammatory responses. In other words, pulmonary fibrosis is a result of abnormal and extended repair and remodelling of damaged lung tissues. We here showed that bleomycin-induced inflammatory responses, such as an increase in BALF leucocyte number and activation of pulmonary MPO, were stimulated in ORP150$^{+/-}$ mice, suggesting that expression of ORP150 could suppress inflammatory responses. As such, we postulated that bleomycin-induced pulmonary fibrosis would be exacerbated in ORP150$^{+/-}$ mice. However, surprisingly, this was not the case. Further to this, we found that increases in pulmonary levels of both active TGF-β1 and myofibroblasts in response to bleomycin were suppressed in ORP150$^{+/-}$ mice compared to wild-type mice. These results suggest that although expression of ORP150 is protective against bleomycin-induced inflammatory responses, it could accentuate pulmonary fibrosis by increasing pulmonary levels of TGF-β1 and myofibroblasts.

As described above, it was recently reported that induction of the ER stress response by chemicals or by expression of misfolded proteins in the ER in alveolar endothelial cells or fibroblasts causes EMT or myofibroblastic differentiation, respectively [18,22]. Therefore, it is possible that the up-regulation of ORP150 expression is responsible for the observed results. We tested this idea *in vitro* and found that the TGF-β1-dependent induction of EMT-like phenotypes in lung epithelial cells was not affected by the suppression of ORP150 expression. On the other hand, the TGF-β1-dependent activation of fibroblasts (myofibroblastic differentiation) was

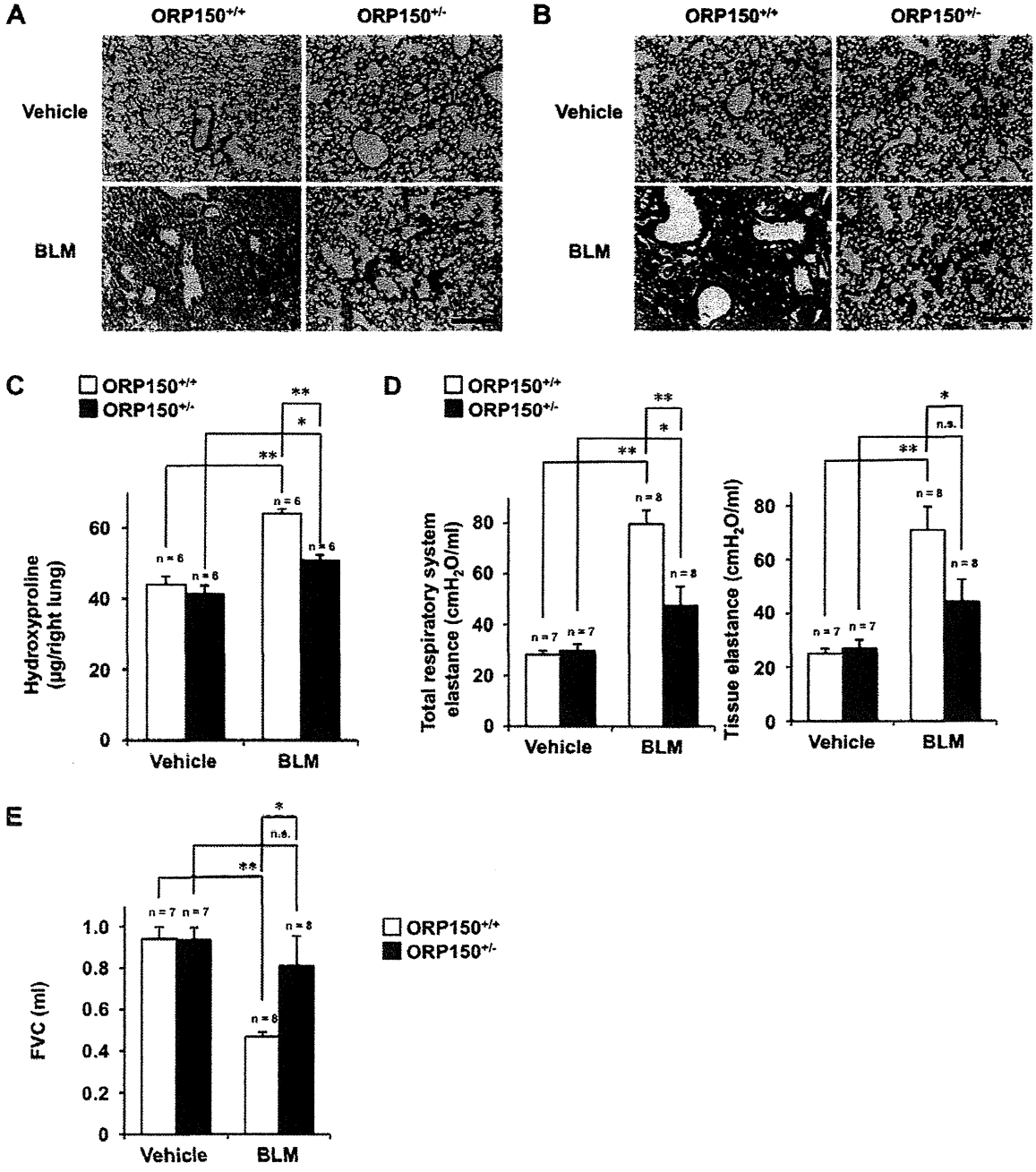

Fig. 3. Effect of down-regulation of ORP150 expression on bleomycin-induced pulmonary fibrosis, alteration of lung mechanics and respiratory dysfunction. ORP150$^{+/-}$ mice and wild-type mice (ORP150$^{+/+}$) were treated with (BLM) or without (Vehicle) bleomycin (5 mg/kg) once-only on day 0 and lung tissue removed on day 14. Sections of pulmonary tissue were subjected to H & E staining (A) or Masson's trichrome staining (B). Pulmonary hydroxyproline levels in lung homogenates were determined (C). Total respiratory system elastance (D), tissue elastance (D) and FVC (E) were determined on day 14. Values shown are mean ± S.E.M. $^{**}p < 0.01$; $^{*}p < 0.05$. Scale bar, 100 μm.

slightly suppressed or stimulated by the suppression or induction, respectively, of ORP150 expression. These results suggest that ORP150 expression stimulates the increase in lung myofibroblasts by stimulating myofibroblastic differentiation rather than by stimulating the EMT of epithelial cells.

Although assessment tools used in bleomycin-induced pulmonary fibrosis are primarily based on histological and quantitative collagen analysis, the clinical management of IPF relies on lung function analysis. We therefore used a computer-controlled small-animal ventilator to monitor the effect of bleomycin on elastance, as an increase in elastance has also been associated with human IPF [29]. We found that the bleomycin-induced alteration of lung mechanics was ameliorated in ORP150$^{+/-}$ mice compared to wild-type mice. An improvement of FVC serves as the endpoint of clinical assessments to estimate the efficacy of candidate drugs in IPF patients; to this extent we found that bleomycin-induced a decrease in FVC was ameliorated in ORP150$^{+/-}$ mice compared to wild-type mice. These results suggest that ORP150 expression stimulates not only bleomycin-induced pulmonary fibrosis but also alters lung mechanics and respiratory dysfunction.

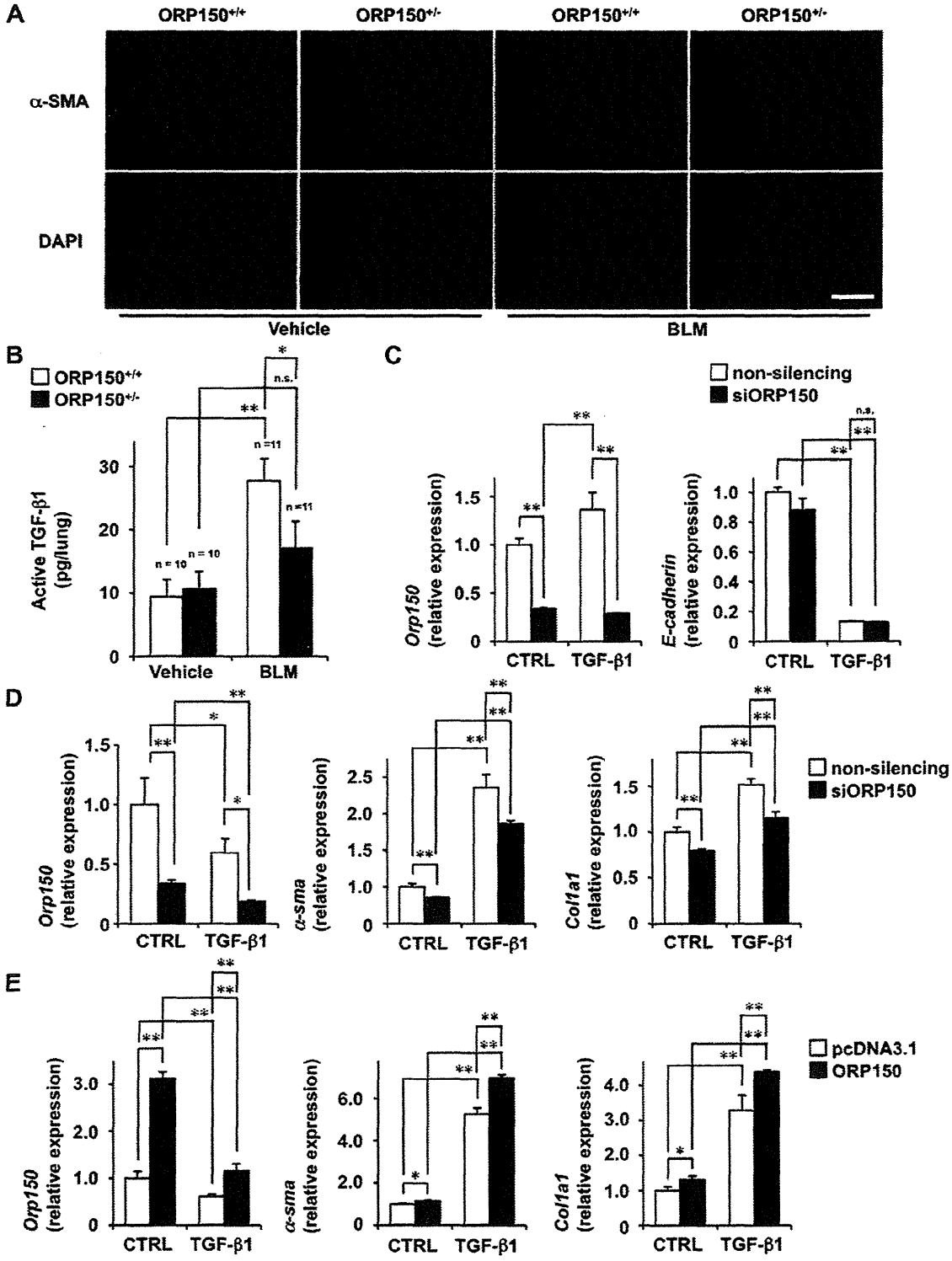

Fig. 4. Effect of down-regulation of ORP150 expression on the pulmonary levels of myofibroblasts and active TGF-β1 *in vivo* and on TGF-β1-induced EMT-like phenotypes of epithelial cells and myofibroblastic differentiation of fibroblasts *in vitro*. (A and B) ORP150$^{+/-}$ mice and wild-type mice (ORP150$^{+/+}$) were treated with (BLM) or without (Vehicle) bleomycin (5 mg/kg) once-only on day 0 and lung tissues removed on day 7 (B) or 14 (A). Sections of pulmonary tissue were subjected to immunohistochemical analysis with an antibody against α-SMA (A). Levels of active TGF-β1 in lung homogenates were measured by ELISA (B). Values shown are mean ± S.E.M. $^{**}p < 0.01$; $^{*}p < 0.05$. Scale bar, 50 μm. (C–E) A549 (C) or HFL-1 (D) cells were transfected with 1.0 μg of siRNA for ORP150 (siORP150) or non-silencing siRNA and incubated for 24 h (C and D). HFL-1 cells were transiently transfected with 2.5 μg of expression plasmid for ORP150 or control vector (pcDNA3.1) and cultured for 24 h (E). Cells were then incubated with 10 ng/ml TGF-β1 for 24 (D and E) or 48 h (C). Total RNA was extracted and subjected to real-time RT-PCR using a specific primer set for each gene. Values were normalised to the *actin gene and expressed relative to the control sample. Values shown are mean ± S.E.M. (n = 3).* $^{**}p < 0.01$; $^{*}p < 0.05$.

Taken together, the findings presented here suggest that ORP150 could serve as a possible drug target for IPF; however, this requires careful examination given that drugs that inhibit ORP150 function may also induce acute lung injury by suppressing the cytoprotective effects that ORP150 exerts against pulmonary damage.

Acknowledgments

This work was supported by Grants-in-Aid for Scientific Research from the Ministry of Health, Labour, and Welfare of Japan, as well as the Japan Science and Technology Agency and Grants-in-Aid for Scientific Research from the Ministry of Education, Culture, Sports, Science and Technology, Japan.

References

[1] American Thoracic Society, Idiopathic pulmonary fibrosis: diagnosis and treatment. International consensus statement. American Thoracic Society (ATS), and the European Respiratory Society (ERS), Am. J. Respir. Crit. Care Med. 161 (2000) 646–664.
[2] D. Sheppard, Transforming growth factor beta: a central modulator of pulmonary and airway inflammation and fibrosis, Proc. Am. Thorac. Soc. 3 (2006) 413–417.
[3] T. Kisseleva, D.A. Brenner, Fibrogenesis of parenchymal organs, Proc. Am. Thorac. Soc. 5 (2008) 338–342.
[4] B.C. Willis, Z. Borok, TGF-beta-induced EMT: mechanisms and implications for fibrotic lung disease, Am. J. Physiol. Lung Cell. Mol. Physiol. 293 (2007) L525–534.
[5] U. Bartram, C.P. Speer, The role of transforming growth factor beta in lung development and disease, Chest 125 (2004) 754–765.
[6] K.K. Kim, M.C. Kugler, P.J. Wolters, L. Robillard, M.G. Galvez, A.N. Brumwell, D. Sheppard, H.A. Chapman, Alveolar epithelial cell mesenchymal transition develops in vivo during pulmonary fibrosis and is regulated by the extracellular matrix, Proc. Natl. Acad. Sci. USA 103 (2006) 13180–13185.
[7] Z. Wu, L. Yang, L. Cai, M. Zhang, X. Cheng, X. Yang, J. Xu, Detection of epithelial to mesenchymal transition in airways of a bleomycin induced pulmonary fibrosis model derived from an alpha-smooth muscle actin-Cre transgenic mouse, Respir. Res. 8 (2007) 1.
[8] R.J. Kaufman, Orchestrating the unfolded protein response in health and disease, J. Clin. Invest. 110 (2002) 1389–1398.
[9] D. Ron, Translational control in the endoplasmic reticulum stress response, J. Clin. Invest. 110 (2002) 1383–1388.
[10] H. Zinszner, M. Kuroda, X. Wang, N. Batchvarova, R.T. Lightfoot, H. Remotti, J.L. Stevens, D. Ron, CHOP is implicated in programmed cell death in response to impaired function of the endoplasmic reticulum, Genes Dev. 12 (1998) 982–995.
[11] T. Hoshino, T. Nakaya, W. Araki, K. Suzuki, T. Suzuki, T. Mizushima, Endoplasmic reticulum chaperones inhibit the production of amyloid-beta peptides, Biochem. J. 402 (2007) 581–589.
[12] T. Namba, T. Hoshino, S. Suemasu, M. Takarada-Iemata, O. Hori, N. Nakagata, A. Yanaka, T. Mizushima, Suppression of expression of endoplasmic reticulum chaperones by *Helicobacter pylori* and its role in exacerbation of non-steroidal anti-inflammatory drug-induced gastric lesions, J. Biol. Chem. 285 (2010) 37302–37313.
[13] K. Kuwabara, M. Matsumoto, J. Ikeda, O. Hori, S. Ogawa, Y. Maeda, K. Kitagawa, N. Imuta, T. Kinoshita, D.M. Stern, H. Yanagi, T. Kamada, Purification and characterization of a novel stress protein, the 150-kDa oxygen-regulated protein (ORP150), from cultured rat astrocytes and its expression in ischemic mouse brain, J. Biol. Chem. 271 (1996) 5025–5032.
[14] K. Ozawa, M. Miyazaki, M. Matsuhisa, K. Takano, Y. Nakatani, M. Hatazaki, T. Tamatani, K. Yamagata, J. Miyagawa, Y. Kitao, O. Hori, Y. Yamasaki, S. Ogawa, The endoplasmic reticulum chaperone improves insulin resistance in type 2 diabetes, Diabetes 54 (2005) 657–663.
[15] T. Nakagomi, O. Kitada, K. Kuribayashi, H. Yoshikawa, K. Ozawa, S. Ogawa, T. Matsuyama, The 150-kilodalton oxygen-regulated protein ameliorates lipopolysaccharide-induced acute lung injury in mice, Am. J. Pathol. 165 (2004) 1279–1288.
[16] W.E. Lawson, P.F. Crossno, V.V. Polosukhin, J. Roldan, D.S. Cheng, K.B. Lane, T.R. Blackwell, C. Xu, C. Markin, L.B. Ware, G.G. Miller, J.E. Loyd, T.S. Blackwell, Endoplasmic reticulum stress in alveolar epithelial cells is prominent in IPF: association with altered surfactant protein processing and herpesvirus infection, Am. J. Physiol. Lung Cell. Mol. Physiol. 294 (2008) L1119–L1126.
[17] M. Korfei, C. Ruppert, P. Mahavadi, I. Henneke, P. Markart, M. Koch, G. Lang, L. Fink, R.M. Bohle, W. Seeger, T.E. Weaver, A. Guenther, Epithelial endoplasmic reticulum stress and apoptosis in sporadic idiopathic pulmonary fibrosis, Am. J. Respir. Crit. Care Med. 178 (2008) 838–846.
[18] H.A. Baek, D.S. Kim, H.S. Park, K.Y. Jang, M.J. Kang, D.G. Lee, W.S. Moon, H.J. Chae, M.J. Chung, Involvement of endoplasmic reticulum stress in myofibroblastic differentiation of lung fibroblasts, Am. J. Respir. Cell Mol. Biol. (2011).
[19] L.M. Nogee, A.E. Dunbar 3rd, S.E. Wert, F. Askin, A. Hamvas, J.A. Whitsett, A mutation in the surfactant protein C gene associated with familial interstitial lung disease, N. Engl. J. Med. 344 (2001) 573–579.
[20] A.Q. Thomas, K. Lane, J. Phillips 3rd, M. Prince, C. Markin, M. Speer, D.A. Schwartz, R. Gaddipati, A. Marney, J. Johnson, R. Roberts, J. Haines, M. Stahlman, J.E. Loyd, Heterozygosity for a surfactant protein C gene mutation associated with usual interstitial pneumonitis and cellular nonspecific interstitial pneumonitis in one kindred, Am. J. Respir. Crit. Care Med. 165 (2002) 1322–1328.
[21] S. Mulugeta, V. Nguyen, S.J. Russo, M. Muniswamy, M.F. Beers, A surfactant protein C precursor protein BRICHOS domain mutation causes endoplasmic reticulum stress, proteasome dysfunction, and caspase 3 activation, Am. J. Respir. Cell Mol. Biol. 32 (2005) 521–530.
[22] H. Tanjore, D.S. Cheng, A.L. Degryse, D.F. Zoz, R. Abdolrasulnia, W.E. Lawson, T.S. Blackwell, Alveolar epithelial cells undergo epithelial-to-mesenchymal transition in response to endoplasmic reticulum stress, J. Biol. Chem. 286 (2011) 30972–30980.
[23] M. Matsuda, T. Hoshino, Y. Yamashita, K. Tanaka, D. Maji, K. Sato, H. Adachi, G. Sobue, H. Ihn, Y. Funasaka, T. Mizushima, Prevention of UVB radiation-induced epidermal damage by expression of heat shock protein 70, J. Biol. Chem. 285 (2010) 5848–5858.
[24] K. Tanaka, K. Sato, K. Aoshiba, A. Azuma, T. Mizushima, Superiority of PC-SOD to other anti-COPD drugs for elastase-induced emphysema and alteration in lung mechanics and respiratory function in mice, Am. J. Physiol. Lung Cell. Mol. Physiol. 302 (2012) L1250–L1261.
[25] K. Tanaka, T. Ishihara, A. Azuma, S. Kudoh, M. Ebina, T. Nukiwa, Y. Sugiyama, Y. Tasaka, T. Namba, K. Sato, Y. Mizushima, T. Mizushima, Therapeutic effect of lecithinized superoxide dismutase on bleomycin-induced pulmonary fibrosis, Am. J. Physiol. Lung Cell. Mol. Physiol. 298 (2010) L348–L360.
[26] K. Tanaka, Y. Tanaka, T. Namba, A. Azuma, T. Mizushima, Heat shock protein 70 protects against bleomycin-induced pulmonary fibrosis in mice, Biochem. Pharmacol. 80 (2010) 920–931.
[27] S. Mima, S. Tsutsumi, H. Ushijima, M. Takeda, I. Fukuda, K. Yokomizo, K. Suzuki, K. Sano, T. Nakanishi, W. Tomisato, T. Tsuchiya, T. Mizushima, Induction of claudin-4 by nonsteroidal anti-inflammatory drugs and its contribution to their chemopreventive effect, Cancer Res. 65 (2005) 1868–1876.
[28] T. Namba, T. Hoshino, K. Tanaka, S. Tsutsumi, T. Ishihara, S. Mima, K. Suzuki, S. Ogawa, T. Mizushima, Up-regulation of 150-kDa oxygen-regulated protein by celecoxib in human gastric carcinoma cells, Mol. Pharmacol. 71 (2007) 860–870.
[29] K. Ask, R. Labiris, L. Farkas, A. Moeller, A. Froese, T. Farncombe, G.B. McClelland, M. Inman, J. Gauldie, M.R. Kolb, Comparison between conventional and "clinical" assessment of experimental lung fibrosis, J. Transl. Med. 6 (2008) 16.

Biochemical Pharmacology 84 (2012) 1470–1481

Contents lists available at SciVerse ScienceDirect

Biochemical Pharmacology

journal homepage: www.elsevier.com/locate/biochempharm

Identification of a unique nsaid, fluoro-loxoprofen with gastroprotective activity☆,☆☆

Shintaro Suemasu [a,b], Naoki Yamakawa [a,b], Tomoaki Ishihara [a], Teita Asano [a], Kayoko Tahara [a], Ken-ichiro Tanaka [a,b], Hirofumi Matsui [c], Yoshinari Okamoto [b], Masami Otsuka [b], Koji Takeuchi [d], Hidekazu Suzuki [e], Tohru Mizushima [a,b,*]

[a] Department of Analytical Chemistry, Faculty of Pharmacy, Keio University, Tokyo 105-8512, Japan
[b] Faculty of Life Sciences, Kumamoto University, Kumamoto 862-0973, Japan
[c] Graduate School of Comprehensive Human Sciences, University of Tsukuba, Tsukuba 305-8575, Japan
[d] Division of Pathological Sciences, Department of Pharmacology and Experimental Therapeutics, Kyoto Pharmaceutical University, Kyoto 607-8414, Japan
[e] Division of Gastroenterology and Hepatology, Department of Internal Medicine, Keio University School of Medicine, Tokyo 160-8582, Japan

ARTICLE INFO

Article history:
Received 6 August 2012
Accepted 18 September 2012
Available online 26 September 2012

Keywords:
NSAIDs
Gastrointestinal complications
Mucus

ABSTRACT

We previously proposed that direct cytotoxicity of NSAIDs due to their membrane permeabilization activity, together with their ability to decrease gastric prostaglandin E_2, contributes to production of gastric lesions. Compared to loxoprofen (LOX), fluoro-loxoprofen (F-LOX) has much lower membrane permeabilization and gastric ulcerogenic activities but similar anti-inflammatory activity. In this study, we examined the mechanism for this low ulcerogenic activity in rats. Compared to LOX, the level of gastric mucosal cell death was lower following administration of F-LOX. However, the gastric level of prostaglandin E_2 was similar in response to treatment with the two NSAIDs. Oral pre-administration of F-LOX conferred protection against the formation of gastric lesions produced by subsequent administration of LOX and orally administered F-LOX resulted in a higher gastric pH value and mucus content. In the presence of a stimulant of gastric acid secretion, the difference in the ulcerogenic activity of F-LOX and LOX was less apparent. Furthermore, an increase in the mucus was observed in gastric cells cultured in the presence of F-LOX in a manner dependent of increase in the cellular level of cAMP. These results suggest that low ulcerogenic activity of F-LOX involves its both low direct cytotoxicity and protective effect against the development of gastric lesions. This protective effect seems to be mediated through an increase in a protective factor (mucus) and a decrease in an aggressive factor (acid).

1. Introduction

The balance between aggressive and defensive factors determines the development of gastric lesions, with either a relative increase in aggressive factors or a decrease in protective factors resulting in lesions. The gastric mucosa can be challenged by a variety of both endogenous and exogenous factors, including gastric acid, reactive oxygen species, ethanol, *Helicobacter pylori* and non-steroidal anti-inflammatory drugs (NSAIDs) [1]. In order to protect the mucosa, the body relies on defence systems such as the production of surface mucus and bicarbonate, and the regulation of gastric mucosal blood flow. Prostaglandin E_2 (PGE_2) also exerts a strong protective effect, inhibiting the secretion of gastric acid and stimulating the production of mucus [2].

NSAIDs, such as indomethacin, comprise a therapeutically valuable family of drugs [3]. An inhibitory effect of NSAIDs on cyclooxygenase (COX) activity is responsible for their anti-inflammatory actions, COX being an enzyme that is essential for

☆ We thank Dr. H. Sakai (University of Toyama, Toyama, Japan) for helpful discussion on the membrane preparation and enzyme assay.
☆☆ This work was supported by Grants-in-Aid of Scientific Research from the Ministry of Health, Labour, and Welfare of Japan, Grants-in-Aid for Scientific Research from the Ministry of Education, Culture, Sports, Science and Technology of Japan, and Grants-in-Aid of the Japan Science and Technology Agency.

Abbreviations: ABTS, 2,2′-azinobis(3-ethylbenzothiazoline-6-sulfonic acid)-$2NH_4$; BAPTA-AM, 1,2-bis(2-aminophenoxy)ethane-*N,N,N′,N′*-tetraacetic acid; COX, cyclooxygenase; DAPI, 4′,6-diamidino-2-phenylindole dihydrochloride; EIA, enzyme immunoassay; ELLA, enzyme-linked lectin-binding assay; F-LOX, fluoro-loxoprofen; FBS, fetal bovine serum; GAPDH, glyceraldehyde-3-phosphate dehydrogenase; H & E, hematoxylin and eosin; IBMX, 3-isobutyl-1-methylxanthine; LOX, loxoprofen; NSAID, non-steroidal anti-inflammatory drug; PG, prostaglandin; RGM1, rat normal gastric epithelial cell line; SD, Sprague-Dawley; SBA, soybean agglutinin; TCA, trichloroacetic acid; TUNEL, terminal deoxynucleotidyl transferase-mediated biotinylated UTP nick end labeling.

* Corresponding author at: Department of Analytical Chemistry, Faculty of Pharmacy, Keio University, 1-5-30, Shibakoen, Minato-ku, Tokyo 105-8512, Japan. Tel./fax: +81 3 5400 2628.
E-mail address: mizushima-th@pha.keio.ac.jp (T. Mizushima).

0006-2952/$ – see front matter © 2012 Elsevier Inc. All rights reserved.
http://dx.doi.org/10.1016/j.bcp.2012.09.016

the synthesis of prostaglandins, which have a strong capacity to induce inflammation. However, as described above, NSAID use is also associated with gastrointestinal complications [4–7], which was thought to result from the inhibition of COX and a decrease in gastric PGE_2 level. In fact, NSAIDs have been reported to stimulate the secretion of gastric acid and inhibit the production of mucus through decreasing gastric PGE_2 level [8,9]. However, it is now believed that the production of gastric lesions by NSAIDs involves additional mechanisms, given that the increased incidence of gastric lesions and the decrease in PGE_2 levels induced by NSAIDs do not always occur in parallel [10,11]. We have recently demonstrated that NSAIDs induce cell death (apoptosis) in cultured gastric mucosal cells and at the gastric mucosa in a manner independent of COX inhibition [12–16]. With regards to the molecular mechanism governing this apoptosis, we have proposed the following pathway. Permeabilization of cytoplasmic membranes by NSAIDs stimulates Ca^{2+} influx and increases intracellular Ca^{2+} levels, which in turn induces the endoplasmic reticulum stress response [12,17,18]. During the course of this response, an apoptosis-inducing transcription factor, C/EBP homologous transcription factor, is induced and, as we have previously shown, this protein is essential for NSAID-induced apoptosis [13,19]. Furthermore, we have proposed that both COX inhibition and gastric mucosal cell death are important for the formation of NSAID-induced gastric lesions *in vivo* [16,20].

In 1991, two subtypes of COX, COX-1 and COX-2, which are responsible for the majority of COX activity at the gastrointestinal mucosa and in tissues subject to inflammation, respectively, were identified [21]. It is therefore not surprising that a reduced incidence of gastroduodenal lesions has been reported following treatment with selective COX-2 inhibitors [22–24]. However, a recently raised issue concerning the use of selective COX-2 inhibitors is the potential risk of cardiovascular thrombotic events [25,26]. This may be due to the fact that prostacyclin, a potent anti-aggregator of platelets and a vasodilator, is mainly produced by COX-2 [27–29]. Therefore, in order to minimize clinical complications, gastric safe NSAIDs other than selective COX-2 inhibitors need to be developed. Based on the hypothesis outlined above, we believe that NSAIDs with lower membrane permeabilization activity would represent an efficacious alternative, even if they had no selectivity for COX-2 [14].

In order to investigate this possibility, we screened for such compounds from a range of clinically used NSAIDs without COX-2 selectivity, and found that the membrane permeabilization activity and direct cytotoxicity of loxoprofen (LOX) (Fig. 1A) was relatively lower than that of the other NSAIDs tested [30]. LOX is a leading NSAID on the Japanese market, being widely used because clinical studies have suggested that it is safer than other traditional (non-selective) NSAIDs [31,32]. LOX is a pro-drug, which is converted (by reduction of the cyclopentanone moiety) to its active metabolite (the *trans*-alcohol metabolite, LOX-OH) by aromatic aldehyde-ketone reductase (Fig. 1A) [33]. We therefore synthesized a series of LOX derivatives, demonstrating that fluoroloxoprofen (F-LOX) (Fig. 1A) has much lower membrane permeabilization and gastric ulcerogenic activities than LOX, but similar anti-inflammatory activity, suggesting that it is likely to be a therapeutically viable drug [34]. We suggested that F-LOX is also a pro-drug, which is converted to its active metabolite (the *trans*-alcohol metabolite, F-LOX-OH (Fig. 1A)), because the inhibitory effect of F-LOX-OH on COX is much more potent than that of F-LOX *in vitro* [34]. Although we concluded that the low membrane permeabilization activity of F-LOX is responsible for its low ulcerogenic activity [34], it remained possible that other mechanisms could also be involved. In this study, we therefore examined the mechanism governing the low ulcerogenic activity of F-LOX. Our results suggest that this effect is mediated not only by the low direct cytotoxicity due to its low membrane permeabilization activity, but also by protection of the gastric mucosa. In contrast to LOX and other NSAIDs, oral administration of F-LOX led to an increase in gastric pH value and mucus, suggesting that these effects are also involved in the low ulcerogenic activity of this drug.

2. Experimental procedures

2.1. Chemicals and animals

LOX, LOX-OH, F-LOX and F-LOX-OH (Fig. 1A) were synthesized in our laboratory as previously described [34]. Methylcellulose and RPMI1640 were obtained from Wako Pure Chemical Industries (Osaka, Japan). Formaldehyde, paraformaldehyde, Alcian blue 8GX, mucin, cycloheximide, histamine, fetal bovine serum (FBS), Dulbecco's modified Eagle's medium nutrient mixture F-12 Ham, 2-methyl-8-(phenylmethoxy)imidazo[1,2-*a*]pyridine-3-acetonitrile (SCH 28080; an inhibitor of gastric H^+,K^+-ATPase), 3-isobutyl-1-methylxanthine (IBMX), omeprazole, forskolin and bovine serum albumin (BSA) were purchased from Sigma (St. Louis, MO). Mayer's hematoxylin, 1% eosin alcohol solution and mounting medium for histochemical analysis (malinol) were from MUTO Pure Chemicals (Tokyo, Japan). Terminal transferase was obtained from Roche Diagnostics (Mannheim, Germany). Biotin 14-ATP and streptavidin-conjugated Alexa Fluor 488 were purchased from Invitrogen (Carlsbad, CA). Mounting medium for the TdT-mediated biotinylated UTP nick end labeling (TUNEL) assay (VECTASHIELD) was from Vector Laboratories, Inc. (Burlingame, CA). 4′,6-diamidino-2-phenylindole dihydrochloride (DAPI) and 1,2-bis(2-aminophenoxy)ethane-*N*,*N*,*N*′,*N*′-tetraacetic acid (BAPTA-AM) were obtained from Dojindo (Kumamoto, Japan). SQ22536 was from CALBIOCHEM (San Diego, CA). ONO-8711 and ONO-AE2-227 were from our laboratory stocks. The prostaglandin E_2 enzyme immunoassay (EIA) kit was purchased from Cayman Chemical (Ann Arbor, MI). cAMP complete ELISA kit was from Enzo Life Sciences (Farmingdale, NY). Horseradish peroxidase-labeled soybean agglutinin (SBA-HRP) was from Seikagaku Biobusiness Co. (Tokyo, Japan). 2,2′-azinobis(3-ethylbenzothiazoline-6-sulfonic acid)-2NH_4 (ABTS) was obtained from KPL (Gaithersburg, MD). The RNeasy Mini kit was from QIAGEN (Valencia, CA), the first-strand cDNA synthesis kit was obtained from Takara (Kyoto, Japan), and iQ SsoFast EvaGreen Supermix was purchased from Bio-Rad (Hercules, CA). Wistar rats (3-week-old males) and Sprague-Dawley (SD) rats (6-week-old males) were obtained from Charles River Laboratories Japan (Yokohama, Japan). Guinea pigs (3-week-old males) were obtained from Japan SLC (Shizuoka, Japan). Animals were housed under conditions of controlled temperature (22–24 °C) and illumination (12 h light cycle starting at 8:00 AM) for 1 week before experiments. The experiments and procedures described here were performed in accordance with the Guide for the Care and Use of Laboratory Animals as adopted and promulgated by the National Institutes of Health, and were approved by the Animal Care Committee of Keio University and Kumamoto University. Totally, we used 287 Wistar rats, 182 SD rats and 4 guinea pigs for all experiments in this study.

2.2. Gastric and small intestinal damage assay

The gastric ulcerogenic response was examined as described previously [20,35] with some modifications. Wistar or SD rats fasted for 18 h were orally administered each NSAID and, after 8 h or 4 h, respectively, the animals were sacrificed, their stomachs were removed, and the gastric mucosal lesion area measured by an observer unaware of the treatment that the animals had received. For Wistar rats, calculation of the scores involved measuring the area of all the lesions in square millimeters and summing the

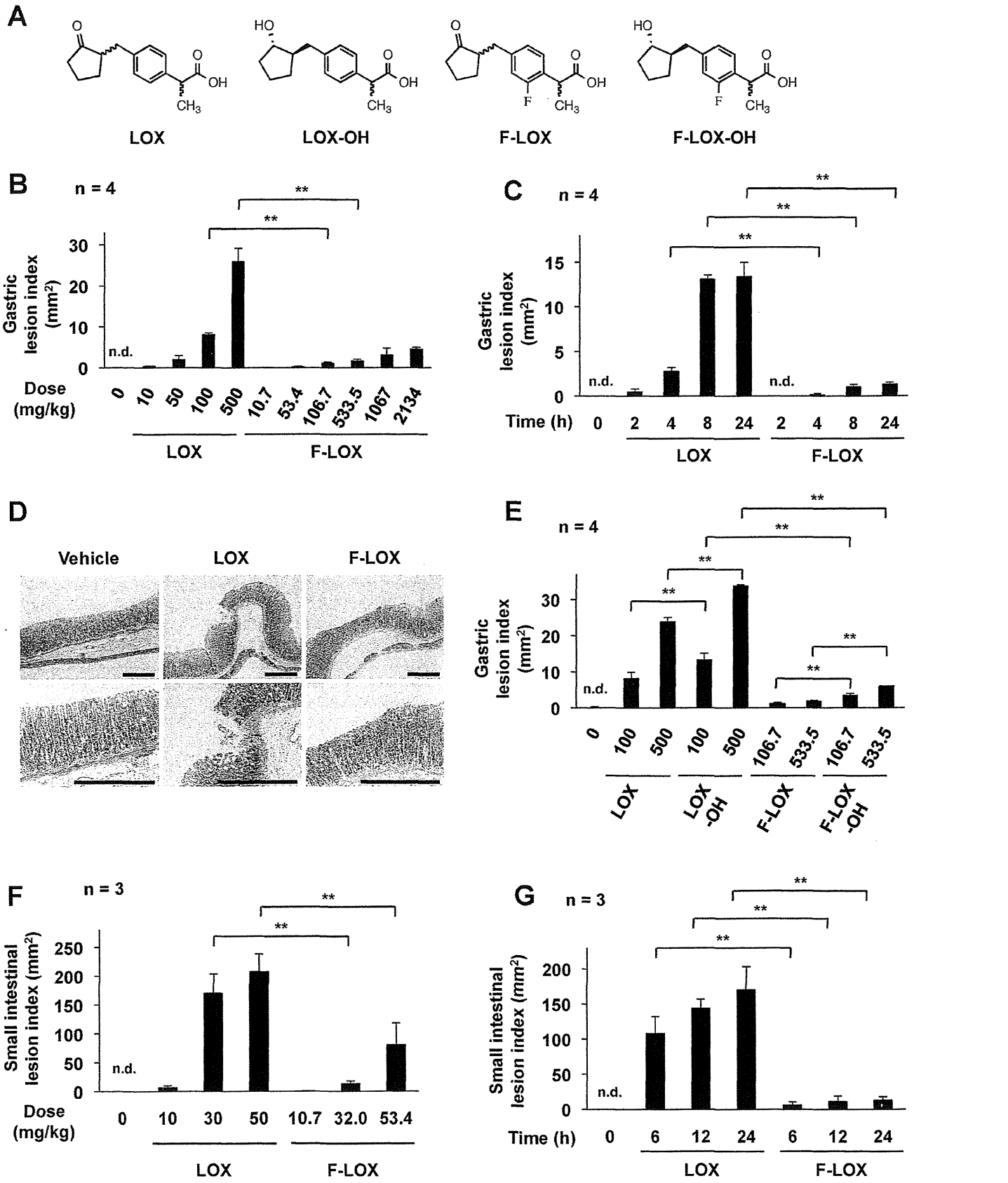

Fig. 1. Production of lesions in the stomach and small intestine by oral administration of F-LOX or LOX. Structures of drugs used in this study were shown (A). Wistar rats were orally administered either the indicated doses (B, E, –F), 200 or 213.4 mg/kg (C and D), or 30 or 32.0 mg/kg (G) of LOX or F-LOX, respectively. Rats were similarly administered LOX-OH or F-LOX-OH (E). Their stomachs (B–E) or small intestines (F, G) were then removed either 8 h later (B, D, E), at the indicated time-points (C, G), or 24 h later (F). The stomach and small intestine were scored for damage (B, C, E, F and G) and sections of gastric tissues were prepared and subjected to H & E staining. Images are magnified 2.5 times (lower panels) (D). Values are mean ± S.E.M. $^{**}P < 0.01$; n.d., not detected. Scale bar, 50 μm.

values to give an overall lesion index. For SD rats, calculation of the scores involved measuring the length of all the lesions in millimeters and summing the values to give an overall gastric lesion index.

The gastric PGE_2 level was determined by EIA according to the manufacturer's instructions.

The intestinal ulcerogenic response was examined as described previously [36,37], with some modifications. LOX or F-LOX was orally administered to unfasted rats and the animals were sacrificed 24 h later. Both the jejunum and ileum were removed and treated with formalin for fixation. Samples were opened along the antimesenteric attachment and the areas of the small intestinal lesions were measured by an observer unaware of the treatment that the animals had received. Calculation of the scores involved measuring the area of all the lesions in square millimeters and summing the values to give an overall small intestinal lesion index.

2.3. Histochemical analysis and TUNEL assay

Wistar rats which had been fasted for 18 h were orally administered LOX or F-LOX and, 8 h later, the animals were sacrificed and their stomachs were removed. Samples were fixed in 4% buffered paraformaldehyde and embedded in paraffin before being cut into 4-μm sections.

For histological examination (hematoxylin and eosin (H&E) staining), the sections were stained first with Mayer's hematoxylin and then with 1% eosin alcohol solution. The samples were mounted with malinol and inspected with the aid of an Olympus BX51 microscope (Tokyo, Japan).

For the TUNEL assay, the sections were incubated first with proteinase K (20 μg/ml) for 15 min at 37 °C, then with TdT and biotin 14-ATP for 1 h at 37 °C, and finally with streptavidin-conjugated Alexa Fluor 488 for 1 h. Samples were mounted with VECTASHIELD and inspected using fluorescence microscopy (KEYENCE BIOREVO, Osaka, Japan).

2.4. Measurement of gastric content volume, gastric pH value and contents of gastric mucin

The gastric pH value and mucus level were measured as previously described [38–40]. SD rats which had been fasted for 18 h were orally administered LOX or F-LOX and, 1 h later, the abdomen was opened and the pylorus was ligated under ether anesthesia. Three hours later, the animals were killed by deep ether anesthesia, the stomach was removed, the gastric contents were collected and its volume was determined. The gastric contents titrated with 10 mM NaOH to pH 7.0 using Twin pH (Horiba, Kyoto, Japan). The gastric acid output was calculated based on the volume of 10 mM NaOH required for neutralization and the gastric content volume.

For determination of mucus content, the gastric contents were incubated with 0.4 mg/ml (final concentration) Alcian blue 8GX for 24 h at 20 °C and then centrifuged. The concentration of Alcian blue in the supernatant was estimated by measuring the optical density at 615 nm. The amount of mucus adhering to the gastric mucosa was also determined, and the sum of the two values used as a measure of the total mucus content.

2.5. Real-time RT-PCR analysis

Total RNA was extracted from gastric tissues and cells using an RNeasy kit according to the manufacturer's protocol. Samples (2.5 μg of RNA) were reverse-transcribed using a first-strand cDNA synthesis kit according to the manufacturer's instructions. Synthesized cDNA was used in real-time RT-PCR (Bio-Rad Chromo 4 system) experiments using SsoFast EvaGreen Supermix, and analyzed with Opticon Monitor software according to the manufacturer's instructions. Specificity was confirmed by electrophoretic analysis of the reaction products and by inclusion of template- or reverse transcriptase-free controls. To normalize the amount of total RNA present in each reaction, glyceraldehyde-3-phosphate dehydrogenase (GAPDH) or actin cDNA was used as an internal standard.

Primers were designed using the Primer3 website. The primers used were (name, forward primer and reverse primer): *muc1*, 5′-agagaccgctactgccattg-3′ and 5′-cagctggacctctttccaac-3′; muc5ac, 5′-aactctgcccaccacaagc-3′ and 5′-tgccatctatccaatcagtccaat-3′; *muc6*, 5′-tgctgtctccagcacaaaac-3′ and 5′-tcagaagtctgcgtcactgc-3′; *gapdh*, 5′-atgtatccgttgtggatctgac-3′ and 5′-cctgcttcaccaccttcttg-3′; *actin*, 5′-gtcgtaccactggcattgtg-3′ and 5′-gctgatcttgcccttgagac-3′.

2.6. Cell culture

A rat normal gastric epithelial cell line (RGM1) [41] was provided by the Riken Cell Bank (Tsukuba, Japan). Cells were cultured in Dulbecco's modified Eagle's medium nutrient mixture F-12 Ham containing 20% FBS, 100 U/ml penicillin, and 100 μg/ml streptomycin on plastic culture plates without collagen coating. Cells were exposed to LOX or F-LOX by replacement of the entire bathing medium. The cAMP level in cells was measured by EIA according to the manufacture's instructions.

2.7. Determination of mucin level in culture medium

The amount of mucin in the culture medium was determined by an enzyme-linked lectin-binding assay (ELLA) as described previously [42]. The culture medium was loaded on polystyrene 96-well ELISA plates (Iwaki) and incubated at 4 °C for 12 h. After washing, each well was incubated with blocking buffer (1% BSA in phosphate-buffered saline) for 2 h at 37 °C. After washing, each well was incubated with SBA solution (1 μg/ml SBA-HRP (lectin) in phosphate-buffered saline) for 1 h at 37 °C. After further washing, each well was finally incubated with 100 μl ABTS solution (1 mM ABTS, 0.1 M citrate buffer (pH 4.0) and 0.03% hydrogen peroxide) for 15 min at room temperature. The optical density at 405 nm was then measured.

2.8. Determination of activities of H^+,K^+-ATPase and adenylate cyclase in membrane fraction

Cytoplasmic membrane fractions were prepared from guinea pig gastric mucosa as described previously [43]. Briefly, the fundic region of the mucosa was scraped and homogenized in 5 mM Tris-HCl (pH 7.4) buffer containing 250 mM sucrose and 1 mM EGTA. The suspension was centrifuged at 800 × *g* for 10 min, and the resultant supernatant was further centrifuged at 100, 000 × *g* for 90 min. The pellet was re-suspended in PBS and used for the assay as membrane fraction.

H^+,K^+-ATPase activity was measured as described previously [44]. Briefly, membrane fraction (100 μg protein) was diluted with 40 mM Tris-HCl (pH 6.8) buffer containing 3 mM $MgSO_4$, 15 mM KCl, 5 mM NaN_3 and 2 mM ouabain and pre-incubated with each tested chemical in the presence or absence of 50 μM SCH 28080 for 30 min at 37 °C. Omeprazole was activated by treatment with Tris-PIPES (pH 5.7) buffer before this incubation. Then, ATP solution (1 mM at the final concentration) was added, incubated for 10 min at 37 °C and the reaction was terminated by the addition of ice-cold stop solution (12% perchloric acid and 3.6% ammonium molybdate). Inorganic phosphate released was measured as previously described [45]. The H^+,K^+-ATPase activity was calculated as the difference between the activities in the presence and absence of SCH 28080.

Adenylate cyclase activity was measured as described previously [46]. Briefly, membrane fraction (100 μg protein, 75 μl) was pre-incubated with each tested chemical in 96 well plates for 5 min at room temperature. Then 25 μl adenylate cyclase assay buffer (final concentrations; 50 mM Tris-HCl (pH 7.4), 100 mM KCl, 10 mM $MgCl_2$, 0.25 mM ATP and 1 mM IBMX) was added, incubated for 30 min at 37 °C and the reaction was terminated by the addition of 100 μl 0.2 N HCl. The cAMP level was measured by EIA according to the manufacture's instructions.

2.9. Statistical analysis

All values are expressed as the mean ± S.E.M. Two-way ANOVA followed by the Tukey test or the Student's *t*-test for unpaired results was used to evaluate differences between more than two groups or between two groups, respectively. Differences were considered to be significant for values of $P < 0.05$.

3. Results

3.1. Comparison between the ulcerogenic response of F-LOX and LOX

The development of gastric lesions following oral administration of F-LOX and LOX to Wistar rats was compared. LOX produced gastric lesions in a dose-dependent manner but F-LOX produced fewer lesions (Fig. 1B). The level of gastric lesions caused by 2134 mg/kg F-LOX (corresponding to 2000 mg/kg LOX, in terms of number of molecules) was lower than that observed with 100 mg/kg LOX, demonstrating that the ulcerogenic activity of F-LOX was less than one-twentieth that of LOX. The time-course for the effect of the two NSAIDs was similar (Fig. 1C), showing that the difference in ulcerogenic activity illustrated in Fig. 1B was not a function of time. Histochemical analysis of gastric sections also revealed that F-LOX caused less gastric mucosal damage than LOX (Fig. 1D). We also examined the ulcerogenic activity of LOX-OH and F-LOX-OH. As shown in Fig. 1E, the ulcerogenic activity of F-LOX-OH was much lower than that of LOX-OH and the activity of LOX-OH or F-LOX-OH was a little more potent than that of LOX or F-LOX, respectively.

We also compared the production of lesions in the small intestine. As shown in Fig. 1F and G, oral administration of F-LOX produced fewer lesions than LOX at all examined time-points. However, the difference between the effect of the two drugs in this case was not as marked as that seen for gastric lesions (Fig. 1B and F).

Both gastric mucosal cell death and a decrease in the gastric level of PGE_2 have been shown to play an important role in the production of gastric lesions by NSAIDs, leading us to compare these processes after oral administration of F-LOX and LOX. The number of TUNEL-positive gastric mucosal cells (level of cell death) was lower in the F-LOX-treated rats (Fig. 2A and B). However, both the dose-response and time-course profiles of the gastric PGE_2 level were similar between the two treatment groups (Fig. 3A and B), suggesting that mucosal cell death rather than gastric PGE_2 level is involved in the lower ulcerogenic activity of F-LOX.

To test this idea, we compared the production of gastric lesions between F-LOX-treated and LOX-treated rats in which the gastric PGE_2 level had been lowered by pre-administration of aspirin (10 mg/kg). This regimen reduced PGE_2 to a negligible level, with subsequent administration of F-LOX or LOX having no effect (Fig. 3 C). As shown in Fig. 3D, the production of gastric lesions in the two treatment groups of rats pre-administered with aspirin was similar to that of control rats, supporting the idea that gastric PGE_2 level is not responsible for the lower ulcerogenic activity of F-LOX compared with LOX.

3.2. Protective effect of orally administered F-LOX on the gastric mucosa

The lower ulcerogenic activity of F-LOX was also observed in SD rats (Fig. 4A), which we used in the following experiments due to

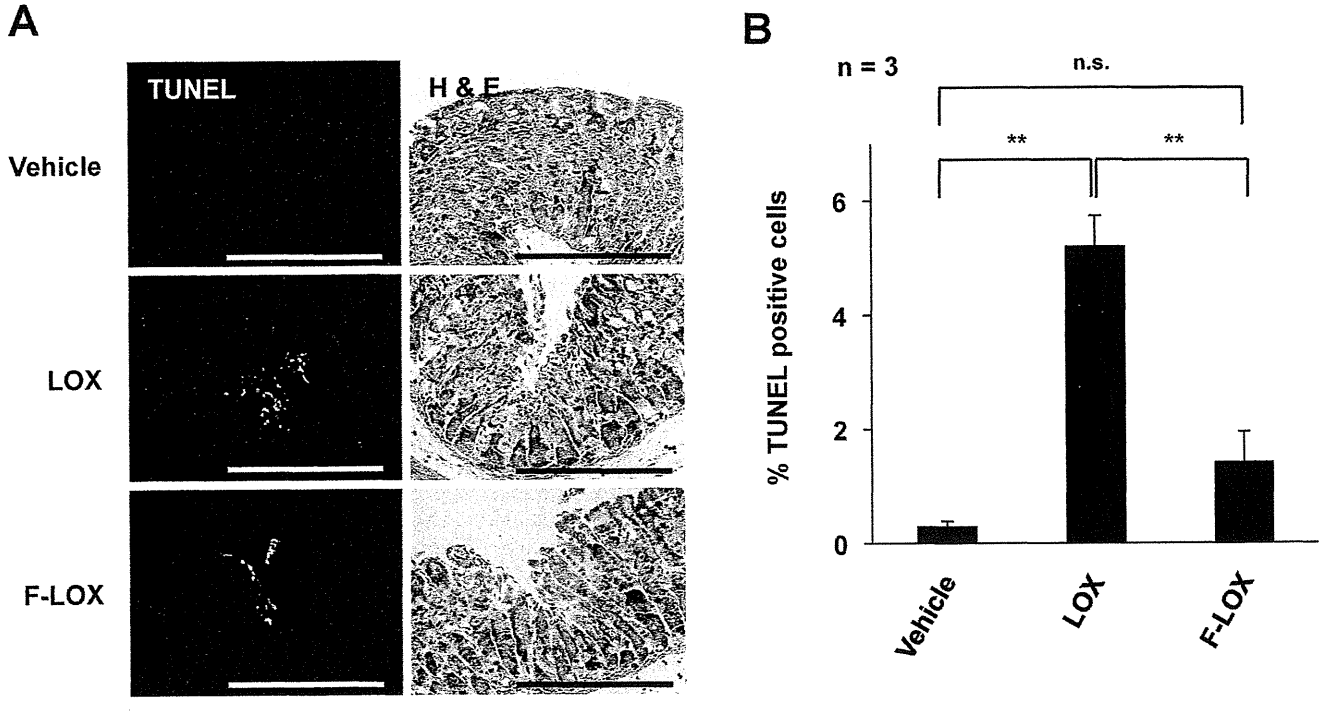

Fig. 2. Gastric mucosal cell death following oral administration of F-LOX or LOX. Wistar rats were orally administered 100 or 106.7 mg/kg of LOX or F-LOX, respectively, and their stomachs were removed 8 h later. A, sections of gastric tissues were prepared and subjected to TUNEL assay, DAPI staining and H & E staining. B, the ratio of TUNEL-positive cells to total cells was determined. Values are mean ± S.E.M. $^{**}P < 0.01$; n.s., not significant. Scale bar, 50 μm.

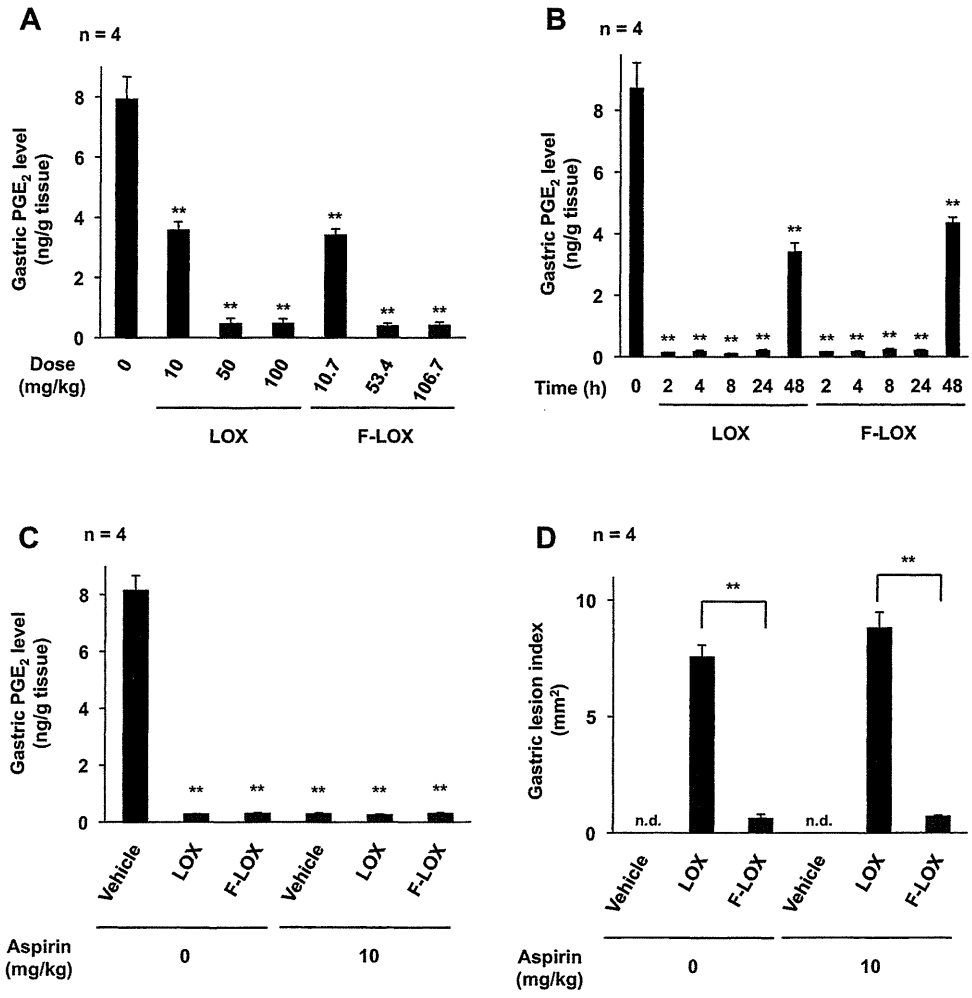

Fig. 3. Decrease in gastric PGE2 level in response to oral administration of F-LOX or LOX. Wistar rats were orally administered either the indicated doses (A), 200 or 213.4 mg/kg (B), or 100 or 106.7 mg/kg (C, D) of LOX or F-LOX, respectively. Rats were orally pre-administered the indicated dose of aspirin, 1 h before NSAID administration (C, D). The stomach was removed either 8 h (A, C, D) or at the indicated time-points (B) after the administration of LOX or F-LOX. A-C, the gastric PGE_2 level was determined by EIA. D, the stomach was scored for damage. Values are mean ± S.E.M. $^{**}P < 0.01$; n.d., not detected.

the availability of established protocols for monitoring gastric pH and mucus level in this strain.

We found that there was no significant difference in the gastric lesions produced by subcutaneous administration of F-LOX and LOX (Fig. 4B). In contrast to treatment with LOX, subcutaneous administration of F-LOX produced more gastric lesions than oral administration (Fig. 4B), although the gastric PGE_2 level in both cases was similar to that obtained following oral administration of the drugs (Fig. 4 C). Surprisingly, we found that oral pre-administration of F-LOX suppressed the production of gastric lesions induced by subsequent oral administration of LOX (Fig. 4D). A similar protective effect of F-LOX was observed for indomethacin-induced gastric lesions (data not shown). As shown in Fig. 4E and F-LOX-OH also showed such a protective effect against LOX-induced gastric lesions. We also found that this protective effect of F-LOX did not occur following its subcutaneous administration (data not shown). These results suggest that the direct interaction of F-LOX (at high concentrations) with the gastric mucosa is somehow protective against NSAID-induced gastric lesions.

3.3. *Mechanism for the protective effect of F-LOX on the gastric mucosa*

To understand the mechanism responsible for the protective effect of F-LOX, we examined the outcome of oral administration of F-LOX or LOX on gastric levels of aggressive (acid) and defensive (mucus) factors. LOX lowered the gastric pH and mucus content (Fig. 5A), phenomena that have been reported with various NSAIDs [8,9]. Surprisingly, oral administration of F-LOX shifted these indexes in the opposite direction, elevating the gastric pH value and mucus content (Fig. 5A). However, subcutaneous administration of F-LOX produced no such effects; subcutaneous administration of both LOX and F-LOX lowered the gastric pH value and mucus content (Fig. 5B).

To understand the mechanism responsible for the increase in the gastric pH value after oral administration of F-LOX, we measured the gastric content volume and determined the gastric acid output. As shown in Fig. 5A, oral administration of F-LOX but not that of LOX increased the gastric content volume, however, both of these drugs similarly increased the gastric acid output. On the other hand, subcutaneous administration of both LOX and F-LOX increased the gastric acid output but did not affect the gastric content volume (Fig. 5B). These results suggest that oral administration of F-LOX increases the gastric pH value through increasing the gastric content volume rather than decreasing the gastric acid output. Supporting this notion, we found that neither LOX nor F-LOX affected the H^+,K^+-ATPase activity in membrane fraction prepared from guinea pig gastric mucosa (Fig. 5C).

To test the contribution of the F-LOX-dependent increase in gastric pH value to the low ulcerogenic activity of this NSAID, we

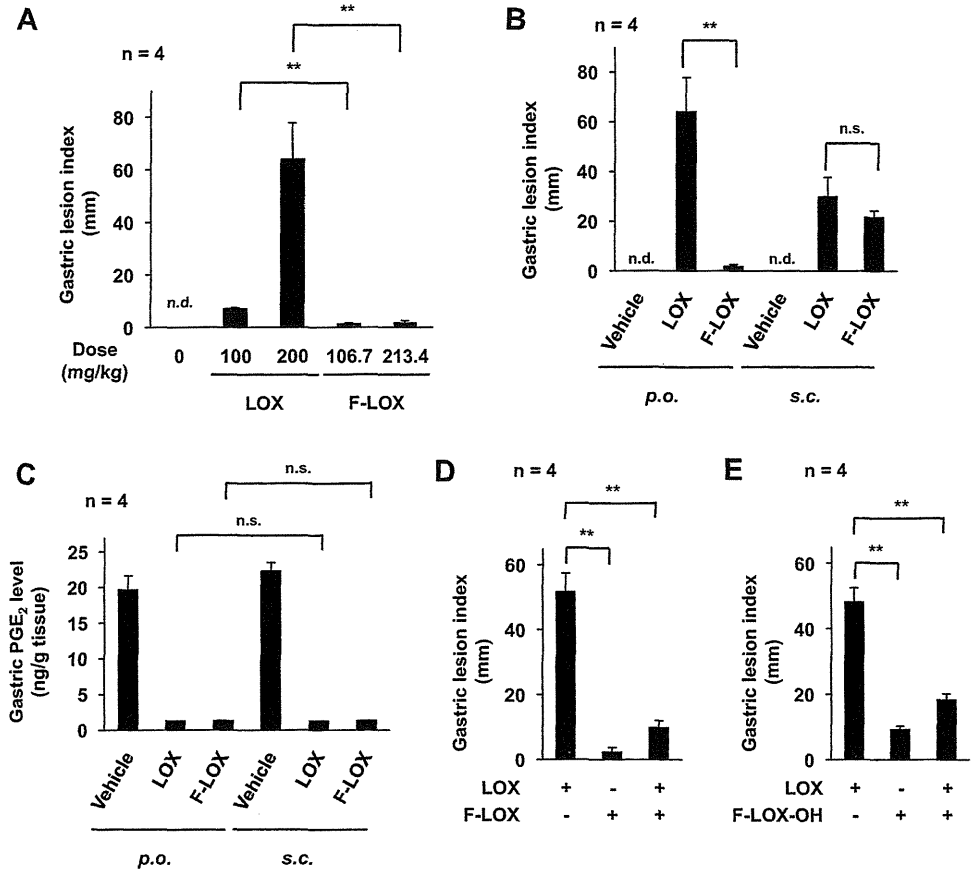

Fig. 4. Protective effect of orally administered F-LOX on the gastric mucosa. (A) SD rats were orally administered the indicated doses of LOX or F-LOX. (B and C) SD rats were orally (*p.o.*) or subcutaneously (*s.c.*) administered 200 or 213.4 mg/kg of LOX or F-LOX, respectively. (D and E) SD rats were orally pre-administered 106.7 mg/kg F-LOX (D) or F-LOX-OH (E), 1 h after which they were orally administered 200 mg/kg of LOX. A, B, D and E, the stomach was removed 4 h after the final administration of the NSAID and scored for damage. C, the gastric PGE_2 level was determined by EIA 4 h after the administration of LOX. Values are mean ± S.E.M. $^{**}P < 0.01$; n.s., not significant; n.d., not detected.

examined the effect of a stimulator of gastric acid secretion (histamine). Pre-administration of 5 mg/kg histamine decreased the pH value in both the presence and absence of subsequent oral administration of F-LOX or LOX (Fig. 6A), as a result of which the extent of the difference in the gastric pH value between the F-LOX- and LOX-treated groups became less apparent (Fig. 6A). As shown in Fig. 6B, F-LOX produced fewer gastric lesions than LOX, even following pre-administration of histamine; however, the extent of this difference was less marked than in the absence of histamine treatment. These results suggest that the higher gastric pH value observed after oral administration of F-LOX is partially responsible for the lower ulcerogenic activity of this NSAID compared with LOX.

3.4. Mechanism for the stimulative effect of F-LOX on the production of mucus

We next examined the effect of oral administration of F-LOX or LOX on the expression levels of mRNAs corresponding to mucin proteins. As shown in Fig. 7A, oral administration of F-LOX or LOX either up-regulated or down-regulated, respectively, the mRNA expression of the *muc1*, *muc5ac* and *muc6* genes (although the down-regulation of *muc6* mRNA by LOX was not statistically significant). We also examined the effect of the two NSAIDs on the production and secretion of mucin *in vitro*, using a rat normal gastric epithelial cell line (RGM1 cells). Treatment of these cells with F-LOX or LOX increased or decreased, respectively, the mucin content in the culture medium (Fig. 7B). Treatment of cells with F-LOX-OH also increased the mucin content in the culture medium (data not shown). To detect the secretion of pre-produced mucin, we examined the effect of F-LOX on the mucin secretion from cells whose protein synthesis was inhibited. Even in this situation, an increase in the mucin content in the culture medium was observed following pre-treatment with a protein synthesis inhibitor, cycloheximide (Fig. 7C), suggesting that the secretion of mucin was stimulated by F-LOX treatment of the cells. On the other hand, treatment of the cells with F-LOX up-regulated the expression levels of mRNAs corresponding to mucin proteins (Fig. 7D). Although there was a trend towards down-regulation of the mRNA expression of these genes following LOX treatment, this effect was not statistically significant (Fig. 7D). Taken together, these results suggest that direct interaction of F-LOX with the gastric mucosa directly stimulates the production and secretion of mucin.

Finally, we addressed the molecular mechanism governing these phenomena. PGE_2 stimulates the production of mucus through both EP_1 and EP_4 receptors [47]. As shown in Fig. 8A, pre-treatment of RGM1 cells with antagonists for EP_1 and EP_4 receptors suppressed PGE_2-induced production of mucin but not F-LOX-induced one (Fig. 8A). EP receptor subtypes are coupled to different intracellular signaling pathways. The EP_1 receptor is coupled to Ca^{2+} mobilization and activation of EP_4 receptor causes activation of adenylate cyclase activity and an increase in the cellular level of cAMP [48]. Thus, we examined the effect of an intracellular Ca^{2+} chelator that is permeable for cytoplasmic membranes (BAPTA-AM) or an inhibitor of adenylate cyclase (SQ22536) on F-LOX-induced production of mucin. As shown in Fig. 8B, pre-treatment of RGM1 cells with SQ22536 but not with BAPTA-AM

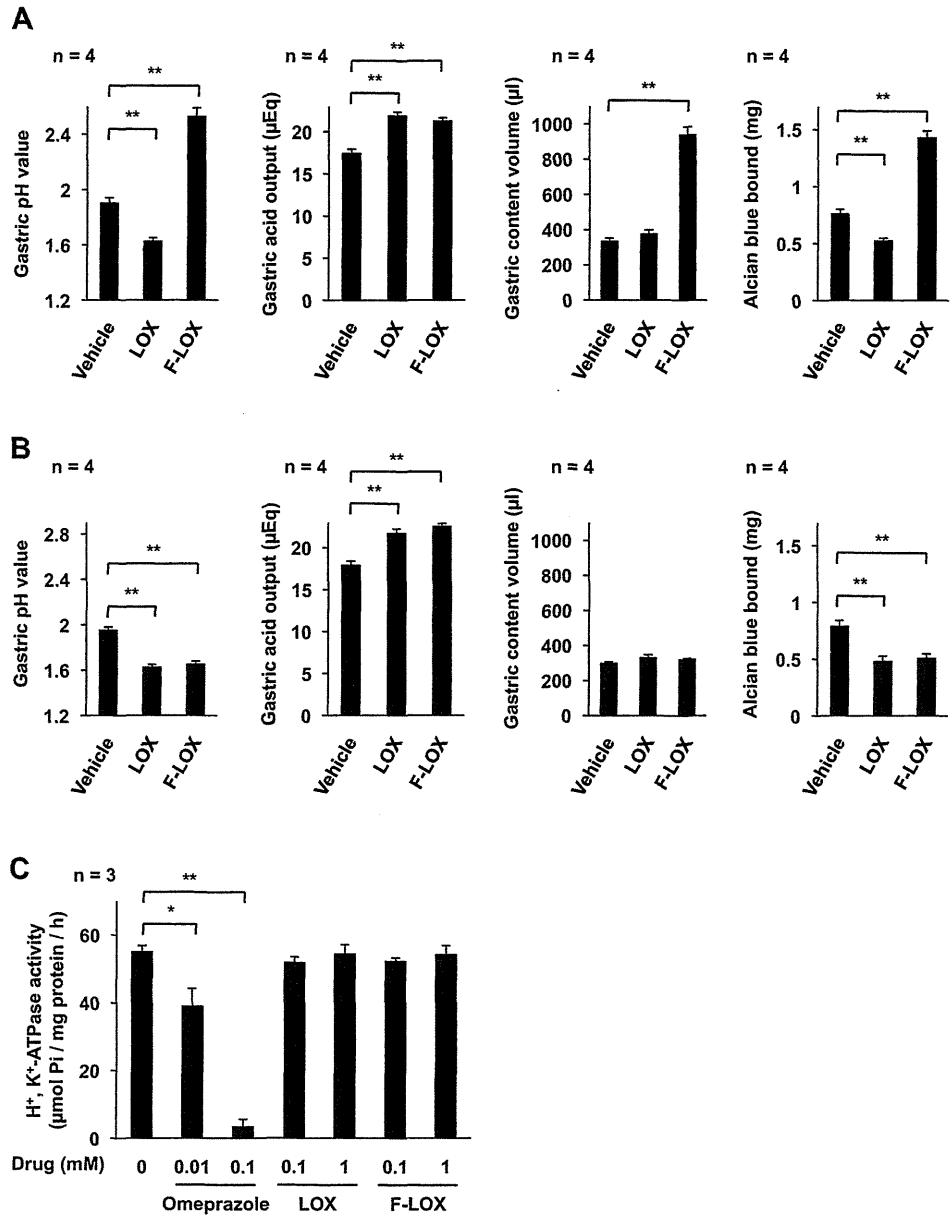

Fig. 5. Effect of F-LOX and LOX on gastric pH and mucus content. SD rats were orally (A) or subcutaneously (B) administered 100 or 106.7 mg/kg of LOX or F-LOX, respectively, 1 h after which the pylorus was ligated and the rats were maintained for a further 3 h. The gastric pH value, gastric acid output, gastric content volume and the amount of mucus in the gastric contents were measured as described in the experimental procedures. (C) Activity of H^+,K^+-ATPase in membrane fraction prepared from guinea pig gastric mucosa was measured in the presence of indicated concentrations of omeprazole (an inhibitor of H^+,K^+-ATPase), LOX or F-LOX as described in the experimental procedures. Values are mean ± S.E.M. $^{**}P < 0.01$; $^{*}P < 0.05$.

suppressed F-LOX-induced production of mucin. We also found that treatment of RGM1 cells with F-LOX increased the cellular level of cAMP to the extent similar to that induced by PGE_2 (Fig. 8C). Since neither LOX nor F-LOX activated adenylate cyclase activity in membrane fraction prepared from guinea pig gastric mucosa (Fig. 8D), F-LOX seems to activate adenylate cyclase indirectly. Furthermore, pre-treatment of cells with SQ22536 suppressed not only PGE_2- but also F-LOX-induced expression levels of mRNAs corresponding to mucin proteins (Fig. 8E). Results in Fig. 8 suggest that direct interaction of F-LOX with the gastric mucosa increases the level of mucin through increase in the cellular level of cAMP.

4. Discussion

F-LOX is a derivative of LOX, which is a leading NSAID on the Japanese market due to its relatively lower incidence of gastrointestinal complications than other traditional NSAIDs [31,32]. The results of a previous study, in which we demonstrated that, compared to LOX, F-LOX has lower ulcerogenic activity but similar anti-inflammatory activity, led us to propose that F-LOX is likely to represent a safer NSAID. However, before this compound can be developed for clinical use, it is first necessary to understand the molecular mechanism governing its low ulcerogenic activity.

In order to address this, we initially determined the dose-response profile of F-LOX, which revealed that its ulcerogenic activity is less than one-twentieth that of LOX when orally administered. Furthermore, the fact that the time-course for the production of gastric lesions observed with F-LOX was similar to that obtained with LOX demonstrated that the former NSAID has lower rather than slower ulcerogenic activity.

We have previously suggested that both gastric mucosal cell death due to the membrane permeabilization activity of NSAIDs and a decrease in the gastric level of PGE_2 due to COX inhibition are

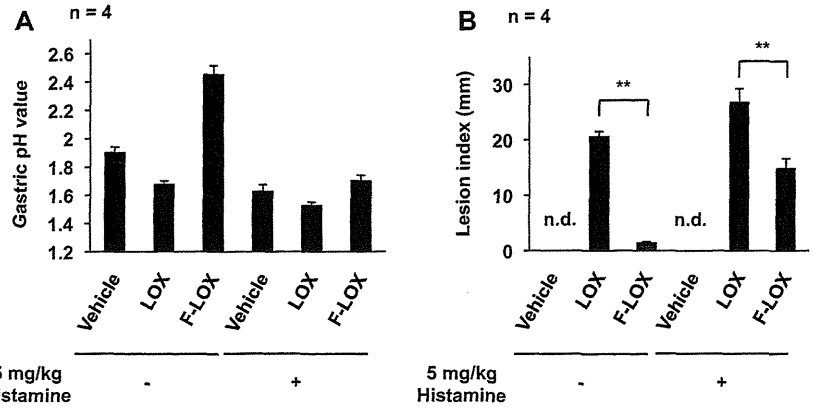

Fig. 6. Effects of pre-administration of histamine on the production of gastric lesions by F-LOX and LOX. SD rats were orally pre-administered the indicated dose of histamine, 1 h after which they were orally administered 100 or 106.7 mg/kg of LOX or F-LOX, respectively. The stomach was then removed 4 h later. A, gastric pH value was determined as described in the legend of Fig. 5. B, the stomach was scored for damage. Values are mean ± S.E.M. $^{**}P < 0.01$; n.d., not detected.

key factors in the production of gastric lesions *in vivo* [16,20]. Based on this hypothesis, NSAIDs without membrane permeabilization activity or those without the ability to decrease the gastric level of PGE_2 (such as COX-2 selective NSAIDs) would represent a therapeutically beneficial option. Among the clinically used NSAIDs that we tested, LOX had the weakest membrane permeabilization activity [30] and, among its derivatives, F-LOX had the weakest such activity [34]. Therefore, it is not surprising that in the current study less gastric mucosal cell death was observed with F-LOX than LOX. Furthermore, as neither LOX nor F-LOX display COX-2 selectivity [34], it is not unexpected that F-LOX decreased the gastric level of PGE_2 to a similar extent to LOX. We also showed that the lower ulcerogenic activity of F-LOX occurred even in the presence of an inhibitor of prostaglandin synthesis (aspirin). Taken together these results led us to conclude that the lower ulcerogenic activity of F-LOX compared with LOX involved gastric mucosal cell death rather than the gastric level of PGE_2.

In contrast to the above findings following oral NSAID administration, the ulcerogenic activities of F-LOX and LOX were indistinguishable when the drugs were administered subcutaneously. It is known that most NSAIDs produce more gastric lesions when administered orally rather than subcutaneously, which is in accordance with what we observed in the case of LOX in the present study. However, F-LOX produced more gastric lesions following subcutaneous administration than following oral administration of the drug. By way of explanation for the opposite effect of F-LOX, we consider a possibility that direct interaction of this NSAID with the gastric mucosa somehow confers a protective effect, but that this protection requires relatively higher concentrations of F-LOX, which can only be achieved by its oral administration. In support of this idea, we found that oral but not subcutaneous pre-administration of F-LOX protected against the formation of gastric lesions induced by subsequent administration of LOX or indomethacin.

A possible explanation for the lower ulcerogenic activity of F-LOX with oral administration than that with subcutaneous administration is that F-LOX but not its active metabolite (F-LOX-OH) confers a protective effect, because we recently found that the conversion of F-LOX to F-LOX-OH occurred very rapidly and the serum level of F-LOX-OH peaked within 1 h after either oral or intravenous administration of F-LOX [49]. However, this idea was ruled out by following observations in this study; the ulcerogenic activity of F-LOX-OH was much lower than that of LOX with their oral administration; oral pre-administration of F-LOX-OH also suppressed the production of gastric lesions induced by subsequent oral administration of LOX; as well as F-LOX (see below), F-LOX-OH increased the level of mucin in culture medium *in vitro*.

In order to understand the molecular mechanism governing the protective activity of F-LOX, we examined the effect of its oral administration on gastric levels of aggressive (acid) and defensive (mucus) factors, demonstrating that the gastric pH value and mucus content were higher following oral administration of the drug. This result is surprising because it is known that PGE_2 inhibits the secretion of acid and stimulates the production of mucus, and therefore that NSAIDs affect these responses in the opposite direction through their inhibitory effects on COX and prostaglandin synthesis [8,9]. This was reflected by the finding that both oral and subcutaneous administration of LOX caused a decrease in gastric pH and mucus. Similarly, in contrast to its oral administration, subcutaneous administration of F-LOX lowered the gastric pH and mucus content. However, the F-LOX-dependent decrease in the gastric level of PGE_2 was indistinguishable following oral and subcutaneous administration, suggesting that orally administered F-LOX, in other words, direct interaction of relatively higher concentrations of F-LOX with the gastric mucosa exerts its protective effects through a COX-independent mechanism.

Oral administration of F-LOX but not that of LOX increased the gastric content volume, however, both of these drugs increased the gastric acid output. On the other hand, subcutaneous administration of both LOX and F-LOX increased the gastric acid output but did not affect the gastric content volume. We also found that neither LOX nor F-LOX affects the H^+,K^+-ATPase activity *in vitro*. These results suggest that direct interaction of relatively higher concentrations of F-LOX with the gastric mucosa increases the gastric pH value through increasing the gastric content volume. However, the mechanism for this increase is unclear at present.

In order to test the contribution of gastric pH value to the production of lesions after oral administration of F-LOX, we examined the effect of a stimulator for gastric acid secretion, histamine. Following oral pre-administration of 5 mg/kg histamine, the difference in gastric pH value in response to oral F-LOX and LOX treatment became less apparent. Similarly, the difference in the production of gastric lesions was reduced, suggesting that the higher gastric pH value contributes to the lower gastric lesion index after oral administration of F-LOX.

We also found that the expression of mRNAs corresponding to mucin proteins was up-regulated not only at the gastric mucosa after oral administration of F-LOX but also in cultured RGM1 cells treated with this NSAID. Furthermore, a F-LOX-dependent increase in the level of mucin was observed in the culture medium, these

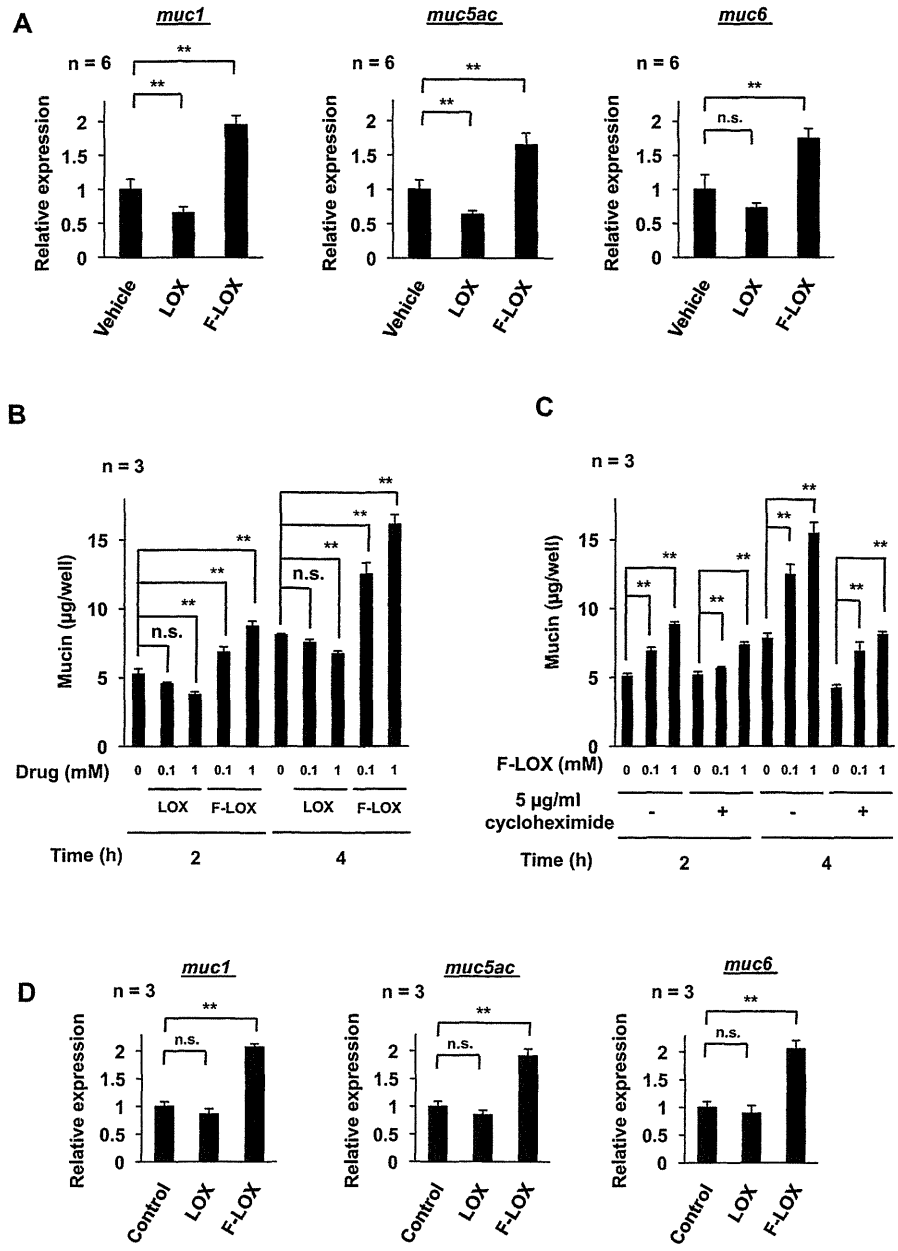

Fig. 7. Effect of F-LOX and LOX on the production and secretion of mucin. (A) SD rats were orally administered 100 or 106.7 mg/kg of LOX or F-LOX, respectively, and the gastric mucosa was removed 4 h later. Total RNA was extracted and subjected to real-time RT-PCR using a specific primer for each gene. Values normalized to the *gapdh* gene are expressed relative to the control sample. (B) RGM1 cells were incubated with the indicated concentrations of LOX or F-LOX for the indicated periods. (C) RGM1 cells were pre-incubated with 5 μg/ml of cycloheximide for 1 h, after which the medium was exchanged to one containing indicated concentrations of F-LOX and cultured the indicated periods. (B and C) The amount of mucin in the culture medium was determined by ELLA. (D) RGM1 cells were incubated with 1 mM of LOX or F-LOX for 4 h. Expression of each mRNA was examined as described above. Values normalized to the *actin* gene are expressed relative to the control sample. Values are mean ± S.E.M. $^{**}P < 0.01$; n.s., not significant.

changes occurring even when the cells were pre-treated with an inhibitor of protein synthesis. These results suggest that F-LOX affects both production and secretion of mucin.

Since PGE_2 stimulates production of mucin through both EP_1 and EP_4 receptors [47], we consider the possibility that F-LOX is an agonist for these receptors. However, this idea was ruled out by the observation that pre-treatment of RGM1 cells with antagonists for EP_1 and EP_4 suppressed PGE_2-induced production of mucin but not F-LOX-induced one. We then tested whether F-LOX directly affects the intracellular signalling pathway coupled with EP_1 or EP_4 receptor (Ca^{2+} mobilization or activation of adenylate cyclase and resulting increase in the cellular level of cAMP, respectively) and found that pre-treatment of RGM1 cells with an inhibitor of adenylate cyclase suppresses F-LOX-dependent increase in the level of mucin and that treatment of cells with F-LOX increases the cellular level of cAMP. Furthermore, we found that pre-treatment of cells with SQ22536 also suppressed F-LOX-induced expression levels of mRNAs corresponding to mucin proteins. These results suggested that F-LOX increases the level of mucin through increase in the cellular level of cAMP.

In line with improvements in diagnostic procedures, it has become clear that NSAIDs induce lesions not only in the stomach but also in the small intestine. However, clinical protocols for the treatment of NSAID-induced lesions of the small intestine have not been established. This is because acid secretion is not as important in the development of these lesions compared with gastric lesions,

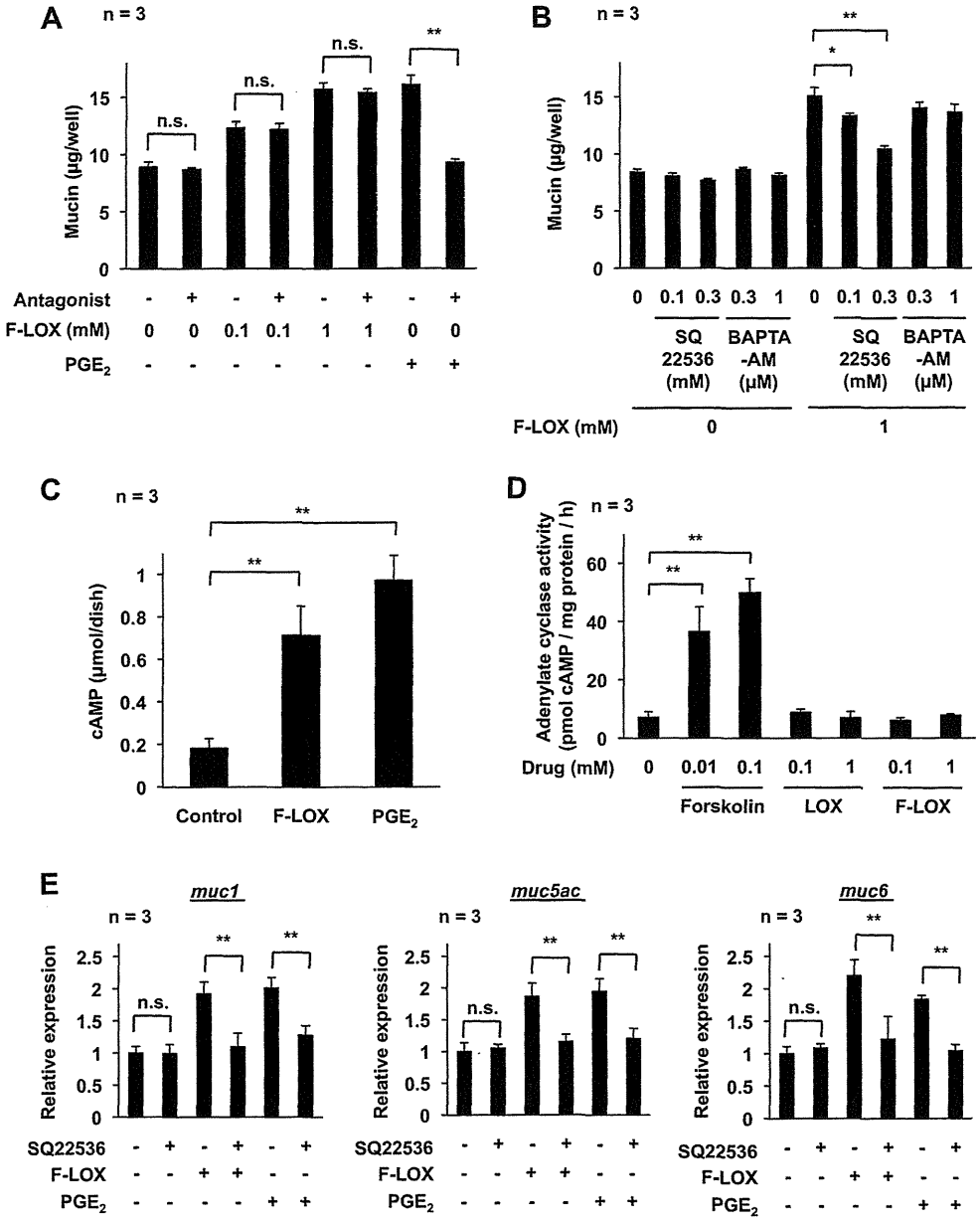

Fig. 8. Molecular mechanism for F-LOX-mediated alteration of production of mucin. RGM1 cells were pre-incubated with 1 μg/ml ONO-8711 (EP_1 antagonist) and 0.1 μg/ml ONO-AE2-227 (EP_4 antagonist) for 0.5 h, after which the medium was exchanged to one containing indicated concentrations of F-LOX and cultured for 4 h (A). RGM1 cells were pre-incubated with the indicated concentrations of SQ22536 (an inhibitor of adenylate cyclase) or BAPTA-AM for 1 h, after which the medium was exchanged to one containing indicated concentrations of F-LOX and cultured for 4 h (B). (A and B) The amount of mucin in the culture medium was determined by ELLA. (C) RGM1 cells were incubated with the indicated concentrations of F-LOX for 0.5 h and cellular cAMP levels were determined by EIA. (D) The activity of adenylate cyclase in membrane fraction prepared from guinea pig gastric mucosa was measured in the presence of indicated concentrations of forskolin (an activator of adenylate cyclase), LOX or F-LOX as described in the experimental procedures. (E) RGM1 cells were pre-incubated with the indicated concentrations of SQ22536 for 1 h, after which the medium was exchanged to one containing indicated concentrations of F-LOX and cultured for 4 h. Expression of each mRNA was examined as described in the legend of Fig. 7. Values are mean ± S.E.M. $^{**}P < 0.01$; $^{*}P < 0.05$; n.s., not significant.

as a result of which acid-controlling drugs are not efficacious [50,51]. In this study, we found that orally administered F-LOX produced fewer small intestine lesions than LOX. Given that the direct cytotoxicity of NSAIDs seems to be involved in, and mucus is protective against, NSAID-induced damage of the small intestine [52,53], this reduced ulcerogenic activity of F-LOX may be the result of its lower cytotoxicity and ability to stimulate mucus synthesis; the development of F-LOX for clinical use is therefore worth considering. However, the extent of the difference between F-LOX and LOX was not as apparent in the small intestine as in the stomach. This may be due to the fact that the pH-increasing activity by F-LOX does not contribute to the suppression of lesion production in the small intestine.

In conclusion, this study has revealed that F-LOX is an unique NSAID, because this NSAID has protective effect against the gastric mucosa and this unique activity contribute to the ulcerogenic activity of this NSAID.

References

[1] Holzer P. Neural emergency system in the stomach. Gastroenterology 1998;114:823–39.
[2] Miller TA. Protective effects of prostaglandins against gastric mucosal damage: current knowledge and proposed mechanisms. Am J Physiol 1983;245: G601–23.
[3] Smalley WE, Ray WA, Daugherty JR, Griffin MR. Nonsteroidal anti-inflammatory drugs and the incidence of hospitalizations for peptic ulcer disease in elderly persons. Am J Epidemiol 1995;141:539–45.

[4] Hawkey CJ. Nonsteroidal anti-inflammatory drug gastropathy. Gastroenterology 2000;119:521–35.
[5] Lichtenberger LM. Where is the evidence that cyclooxygenase inhibition is the primary cause of nonsteroidal anti-inflammatory drug (NSAID)-induced gastrointestinal injury. Topical injury revisited. Biochem Pharmacol 2001;61:631–7.
[6] Whittle BJ. New dogmas or old. Gut 2003;52:1379–81.
[7] Gupta M, Eisen GM. NSAIDs and the gastrointestinal tract. Curr Gastroenterol Rep 2009;11:345–53.
[8] Levine RA, Schwartzel EH. Effect of indomethacin on basal and histamine stimulated human gastric acid secretion. Gut 1984;25:718–22.
[9] Phillipson M, Johansson ME, Henriksnas J, Petersson J, Gendler SJ, Sandler S, et al. The gastric mucus layers: constituents and regulation of accumulation. Am J Physiol Gastrointest Liver Physiol 2008;295:G806–12.
[10] Ligumsky M, Golanska EM, Hansen DG, Kauffman GJ. Aspirin can inhibit gastric mucosal cyclo-oxygenase without causing lesions in rat. Gastroenterology 1983;84:756–61.
[11] Ligumsky M, Sestieri M, Karmeli F, Zimmerman J, Okon E, Rachmilewitz D. Rectal administration of nonsteroidal antiinflammatory drugs Effect on rat gastric ulcerogenicity and prostaglandin E2 synthesis. Gastroenterology 1990;1245–9.
[12] Tanaka K, Tomisato W, Hoshino T, Ishihara T, Namba T, Aburaya M, et al. Involvement of Intracellular Ca2+ Levels in Nonsteroidal Anti-inflammatory Drug-induced Apoptosis. J Biol Chem 2005;280:31059–67.
[13] Tsutsumi S, Gotoh T, Tomisato W, Mima S, Hoshino T, Hwang HJ, et al. Endoplasmic reticulum stress response is involved in nonsteroidal anti-inflammatory drug-induced apoptosis. Cell Death Differ 2004;11:1009–16.
[14] Tomisato W, Tanaka K, Katsu T, Kakuta H, Sasaki K, Tsutsumi S, et al. Membrane permeabilization by non-steroidal anti-inflammatory drugs. Biochem Biophys Res Commun 2004;323:1032–9.
[15] Tomisato W, Tsutsumi S, Rokutan K, Tsuchiya T, Mizushima T. NSAIDs induce both necrosis and apoptosis in guinea pig gastric mucosal cells in primary culture. Am J Physiol Gastrointest Liver Physiol 2001;281:G1092–100.
[16] Aburaya M, Tanaka K, Hoshino T, Tsutsumi S, Suzuki K, Makise M, et al. Heme oxygenase-1 protects gastric mucosal cells against non-steroidal anti-inflammatory drugs. J Biol Chem 2006;281:33422–32.
[17] Tsutsumi S, Namba T, Tanaka KI, Arai Y, Ishihara T, Aburaya M, et al. Celecoxib upregulates endoplasmic reticulum chaperones that inhibit celecoxib-induced apoptosis in human gastric cells. Oncogene 2006;25:1018–29.
[18] Namba T, Hoshino T, Tanaka K, Tsutsumi S, Ishihara T, Mima S, et al. Up-regulation of 150-kDa oxygen-regulated protein by celecoxib in human gastric carcinoma cells. Mol Pharmacol 2007;71:860–70.
[19] Ishihara T, Hoshino T, Namba T, Tanaka K, Mizushima T. Involvement of up-regulation of PUMA in non-steroidal anti-inflammatory drug-induced apoptosis. Biochem Biophys Res Commun 2007;356:711–7.
[20] Tomisato W, Tsutsumi S, Hoshino T, Hwang HJ, Mio M, Tsuchiya T, et al. Role of direct cytotoxic effects of NSAIDs in the induction of gastric lesions. Biochem Pharmacol 2004;67:575–85.
[21] Vane J. Towards a better aspirin. Nature 1994;367:215–6.
[22] Silverstein FE, Faich G, Goldstein JL, Simon LS, Pincus T, Whelton A, et al. Gastrointestinal toxicity with celecoxib vs nonsteroidal anti-inflammatory drugs for osteoarthritis and rheumatoid arthritis: the CLASS study: A randomized controlled trial. Celecoxib Long-term Arthritis Safety Study. JAMA 2000;284:1247–55.
[23] Bombardier C, Laine L, Reicin A, Shapiro D, Burgos VR, Davis B, et al. Comparison of upper gastrointestinal toxicity of rofecoxib and naproxen in patients with rheumatoid arthritis. VIGOR Study Group. N Engl J Med 2000;343:1520–8. 2 p following 8.
[24] FitzGerald GA, Patrono C. The coxibs, selective inhibitors of cyclooxygenase-2. N Engl J Med 2001;345:433–42.
[25] Mukherjee D, Nissen SE, Topol EJ. Risk of cardiovascular events associated with selective COX-2 inhibitors. JAMA 2001;286:954–9.
[26] Mukherjee D. Selective cyclooxygenase-2 (COX-2) inhibitors and potential risk of cardiovascular events. Biochem Pharmacol 2002;63:817–21.
[27] McAdam BF, Catella LF, Mardini IA, Kapoor S, Lawson JA, FitzGerald GA. Systemic biosynthesis of prostacyclin by cyclooxygenase (COX)-2: the human pharmacology of a selective inhibitor of COX-2. Proc Natl Acad Sci USA 1999;96:272–7.
[28] Catella LF, McAdam B, Morrison BW, Kapoor S, Kujubu D, Antes L, et al. Effects of specific inhibition of cyclooxygenase-2 on sodium balance, hemodynamics, and vasoactive eicosanoids. J Pharmacol Exp Ther 1999;289:735–41.
[29] Belton O, Byrne D, Kearney D, Leahy A, Fitzgerald DJ. Cyclooxygenase-1 and -2-dependent prostacyclin formation in patients with atherosclerosis. Circulation 2000;102:840–5.
[30] Yamakawa N, Suemasu S, Kimoto A, Arai Y, Ishihara T, Yokomizo K, et al. Low direct cytotoxicity of loxoprofen on gastric mucosal cells. Biol Pharm Bull 2010;33:398–403.
[31] Misaka E, Yamaguchi T, Iizuka Y, Kamoshida K, Kojima T, Kobayashi K, et al. Anti-inflammatory, Analgesic and Antipyretic Activities of Sodium 2-[4-(2-oxocyclopentan-1-ylmethyl)phenyl] Propionate Dihydrate (CS-600)*. Pharmacometrics 1981;21:753–71.
[32] Kawano S, Tsuji S, Hayashi N, Takei Y, Nagano K, Fusamoto H, et al. Effects of loxoprofen sodium, a newly synthesized non-steroidal anti-inflammatory drug, and indomethacin on gastric mucosal haemodynamics in the human. J Gastroenterol Hepatol 1995;10:81–5.
[33] Sugimoto M, Kojima T, Asami M, Iizuka Y, Matsuda K. Inhibition of prostaglandin production in the inflammatory tissue by loxoprofen-Na, an anti-inflammatory prodrug. Biochem Pharmacol 1991;42:2363–8.
[34] Yamakawa N, Suemasu S, Matoyama M, Kimoto A, Takeda M, Tanaka K, et al. Properties and synthesis of 2-{2-fluoro (or bromo)-4-[(2-oxocyclopentyl)-methyl]phenyl}propanoic acid: nonsteroidal anti-inflammatory drugs with low membrane permeabilizing and gastric lesion-producing activities. J Med Chem 2010;53:7879–82.
[35] Takeuchi K, Ueki S, Okabe S. Importance of gastric motility in the pathogenesis of indomethacin-induced gastric lesions in rats. Dig Dis Sci 1986;31:1114–22.
[36] Tanaka A, Matsumoto M, Hayashi Y, Takeuchi K. Functional mechanism underlying cyclooxygenase-2 expression in rat small intestine following administration of indomethacin: relation to intestinal hypermotility. J Gastroenterol Hepatol 2005;20:38–45.
[37] Asano T, Tanaka K, Yamakawa N, Adachi H, Sobue G, Goto H, et al. HSP70 confers protection against indomethacin-induced lesions of the small intestine. J Pharmacol Exp Ther 2009;330:458–67.
[38] Filaretova L, Tanaka A, Miyazawa T, Kato S, Takeuchi K. Mechanisms by which endogenous glucocorticoid protects against indomethacin-induced gastric injury in rats. Am J Physiol Gastrointest Liver Physiol 2002;283:G1082–89.
[39] Anson ML. The estimation of pepsin, trypsin, papain, and cathepsin with hemoglobin. J Gen Physiol 1938;22:79–89.
[40] Bolton JP, Palmer D, Cohen MM. Stimulation of mucus and nonparietal cell secretion by the E2 prostaglandins. Am J Dig Dis 1978;23:359–64.
[41] Kobayashi I, Kawano S, Tsuji S, Matsui H, Nakama A, Sawaoka H, et al. RGM1, a cell line derived from normal gastric mucosa of rat. In Vitro Cell Dev Biol Anim 1996;32:259–61.
[42] Ohara S, Watanabe T, Hotta K. Comparative study of carbohydrate portion of gastrointestinal mucins using enzyme-linked lectin-binding assay (ELLA). Comp Biochem Physiol B Biochem Mol Biol 1997;116:167–72.
[43] Fujii T, Takahashi Y, Ikari A, Morii M, Tabuchi Y, Tsukada K, et al. Functional association between K + -Cl- cotransporter-4 and H+,K + -ATPase in the apical canalicular membrane of gastric parietal cells. J Biol Chem 2009;284:619–29.
[44] Fujii T, Ohira Y, Itomi Y, Takahashi Y, Asano S, Morii M, et al. Inhibition of P-type ATPases by [(dihydroindenyl)oxy]acetic acid (DIOA), a K+ -Cl- cotransporter inhibitor. Eur J Pharmacol 2007;560:123–6.
[45] Yoda A, Hokin LE. On the reversibility of binding of cardiotonic steroids to a partially purified (Na + K)-activated adenosinetriphosphatase from beef brain. Biochem Biophys Res Commun 1970;40:880–6.
[46] Oner SS, Kaya AI, Onaran HO, Ozcan G, Ugur O. Beta2-Adrenoceptor, Gs and adenylate cyclase coupling in purified detergent-resistant, low density membrane fractions. Eur J Pharmacol 2010;630:42–52.
[47] Ohnishi A, Shimamoto C, Katsu K, Ito S, Imai Y, Nakahari T. EP1 and EP4 receptors mediate exocytosis evoked by prostaglandin E(2) in guinea-pig antral mucous cells. Exp Physiol 2001;86:451–60.
[48] Coleman RA, Smith WL, Narumiya S. International Union of Pharmacology classification of prostanoid receptors: properties, distribution, and structure of the receptors and their subtypes. Pharmacol Rev 1994;46:205–29.
[49] Yamakawa N, Suemasu S, Watanabe H, Tahara K, Tanaka KI, Okamoto Y, et al. Comparison of pharmacokinetics between loxoprofen and its derivative with lower ulcerogenic activity, fluoro-loxoprofen. Drug Metab Pharmacokinet 2012.
[50] Goldstein JL, Eisen GM, Lewis B, Gralnek IM, Aisenberg J, Bhadra P, et al. Small bowel mucosal injury is reduced in healthy subjects treated with celecoxib compared with ibuprofen plus omeprazole, as assessed by video capsule endoscopy. Aliment Pharmacol Ther 2007;25:1211–22.
[51] Aabakken L, Bjornbeth BA, Weberg R, Viksmoen L, Larsen S, Osnes M. NSAID-associated gastroduodenal damage: does famotidine protection extend into the mid- and distal duodenum. Aliment Pharmacol Ther 1990;4:295–303.
[52] Somasundaram S, Sigthorsson G, Simpson RJ, Watts J, Jacob M, Tavares IA, et al. Uncoupling of intestinal mitochondrial oxidative phosphorylation and inhibition of cyclooxygenase are required for the development of NSAID-enteropathy in the rat. Aliment Pharmacol Ther 2000;14:639–50.
[53] Basivireddy J, Vasudevan A, Jacob M, Balasubramanian KA. Indomethacin-induced mitochondrial dysfunction and oxidative stress in villus enterocytes. Biochem Pharmacol 2002;64:339–49.

See related commentary on pg 868

ORIGINAL ARTICLE

Suppression of UV-Induced Wrinkle Formation by Induction of HSP70 Expression in Mice

Minoru Matsuda[1,2,3], Tatsuya Hoshino[1], Naoki Yamakawa[1,2], Kayoko Tahara[1], Hiroaki Adachi[4], Gen Sobue[4], Daisuke Maji[3], Hironobu Ihn[2] and Tohru Mizushima[1]

UV-induced wrinkle formation owing to the degeneration of the extracellular matrix (ECM) is a major dermatological problem in which abnormal activation of matrix metalloproteinases (MMPs) and elastases have important roles. Heat shock protein 70 (HSP70) has cytoprotective and anti-inflammatory activities. In this study, we examined the effect of HSP70 expression on UV-induced wrinkle formation. Mild heat treatment (exposure to heated water at 42 °C) of the dorsal skin of hairless mice induced the expression of HSP70. The long-term repeated exposure to UV induced epidermal hyperplasia, decreased skin elasticity, degeneration of ECM, and wrinkle formation, which could be suppressed in mice concomitantly subjected to this heat treatment. The UV-induced epidermal hyperplasia, decreased skin elasticity, and degeneration of ECM were less apparent in transgenic mice expressing HSP70 than in wild-type mice. UV-induced fibroblast cell death, infiltration of inflammatory cells, and activation of MMPs and elastase in the skin were also suppressed in the transgenic mice. This study provides evidence for an inhibitory effect of HSP70 on UV-induced wrinkle formation. The results suggest that this effect is mediated by various properties of HSP70, including its cytoprotective and anti-inflammatory activities. We propose that HSP70 inducers used in a clinical context could prove beneficial for the prevention of UV-induced wrinkle formation.

Journal of Investigative Dermatology (2013) **133,** 919–928; doi:10.1038/jid.2012.383; published online 25 October 2012

INTRODUCTION

The skin is damaged by various environmental stressors, especially by long-term chronic solar UV radiation (photoaging). UV light can be separated according to wavelength, with UVB thought to have an important role in photoaging (Matsumura and Ananthaswamy, 2004; Rabe *et al.*, 2006). This process is mediated not only by direct UV-induced damage to the skin but also indirectly via the induction of inflammation and production of reactive oxygen species that are released from infiltrated leukocytes (Rabe *et al.*, 2006).

Both wrinkle formation and skin hyperpigmentation disorders are major dermatological problems. It is believed that epidermal hyperplasia owing to epidermal damage and inflammation, as well as alteration of the extracellular matrix (ECM) (such as damage to collagen fibers, suppression of collagen expression, disruption and degeneration of elastic fibers, and disruption of the epidermal basal membrane), has an important role in UV-induced wrinkle formation and decreased skin elasticity, which is closely linked to wrinkle formation (Talwar *et al.*, 1995; Imokawa, 2009; Rijken and Bruijnzeel, 2009). As these UV-induced phenomena can be reproduced to some extent in hairless mice exposed to long-term repeated exposure to UVB radiation, this animal model has been used to examine the mechanism of UV-induced wrinkle formation (Schwartz, 1988).

Matrix metalloproteinases (MMPs)-dependent qualitative and quantitative decreases in the ECM have an important role in UV-induced wrinkle formation. The activities of MMP-1, 2, 3, and 9 were increased by UVB irradiation in mouse and human skin (Inomata *et al.*, 2003; Rabe *et al.*, 2006), whereas the topical treatment of mouse skin with MMP inhibitors blocked UV-induced wrinkle formation, and decreased skin elasticity and basal membrane disruption (Inomata *et al.*, 2003). In mouse, MMP-2, 8, and 13, or MMP-2 and 9, are responsible for the degradation of collagen types I or IV, respectively, which constitute dermal collagen fibers or the epidermal basal membrane, respectively (Aimes and Quigley, 1995; Visse and Nagase, 2003; Kessenbrock *et al.*, 2010). In addition to collagenases (MMP-8 and 13), gelatinases (MMP-2 and 9) have important roles in UV-induced wrinkle formation, decreased skin elasticity, and basal membrane disruption (Inomata *et al.*, 2003). Tissue inhibitors of MMPs (TIMPs) also have important roles in these phenomena. The disruption

[1]*Department of Analytical Chemistry, Faculty of Pharmacy, Keio University, Tokyo, Japan;* [2]*Graduate School of Medical and Pharmaceutical Sciences, Kumamoto University, Kumamoto, Japan;* [3]*Saishunkan Pharmaceutical, Kumamoto, Japan and* [4]*Nagoya University Graduate School of Medicine, Nagoya, Japan*

Correspondence: Tohru Mizushima, Department of Analytical Chemistry, Faculty of Pharmacy, Keio University, Tokyo 105-8512, Japan. E-mail: mizushima-th@pha.keio.ac.jp

Abbreviations: ECM, extracellular matrix; HSPs, heat shock proteins; MMPs, matrix metalloproteinases; TIMPs, tissue inhibitors of MMPs

Received 30 November 2011; revised 23 July 2012; accepted 6 August 2012; published online 25 October 2012

and degeneration of elastic fibers also have an important role in wrinkle formation and decreased skin elasticity (Imokawa, 2009). To this extent, the topical application of elastase inhibitors significantly suppressed UV-induced wrinkle formation in hairless mice (Tsuji *et al.*, 2001; Tsukahara *et al.*, 2001; Zhao *et al.*, 2009).

Induction of the expression of heat shock proteins (HSPs), especially that of HSP70, provides resistance to stressors (Morimoto and Santoro, 1998). In addition to this cytoprotective effect, HSP70 has an anti-inflammatory activity (Krappmann *et al.*, 2004; Chen *et al.*, 2006; Tang *et al.*, 2007; Weiss *et al.*, 2007). The artificial expression of HSP70 in keratinocytes and melanocytes confers protection *in vitro* against UV (Maytin *et al.*, 1994; Trautinger *et al.*, 1995; Park *et al.*, 2000; Wilson *et al.*, 2000; Trautinger, 2001). However, the role of HSP70 in photoaging *in vivo* remains unclear. We recently showed that UV-induced skin damage and the resulting inflammatory responses were suppressed in transgenic mice expressing HSP70 (Matsuda *et al.*, 2010). We also reported that UV-induced melanin production by the skin was suppressed in transgenic mice expressing HSP70 (Hoshino *et al.*, 2010). However, the role of HSP70 in UV-induced wrinkle formation is yet to be elucidated.

In this study, we examine the effect of the expression of HSP70 on UV-induced wrinkle formation and decreased skin elasticity. UV-induced epidermal hyperplasia, decreased skin elasticity, and wrinkle formation were suppressed in hairless mice concomitantly subjected to mild heat treatment (exposure to heated water at 42 °C). Moreover, UV-induced epidermal hyperplasia, decreased skin elasticity, the disruption of collagen and elastic fibers, and the basal membrane of the epidermis, and activation of MMPs and elastase were significantly suppressed in transgenic mice expressing HSP70 compared with wild-type mice. These results suggest that HSP70 expression protects the skin against UV-induced wrinkle formation.

RESULTS

Effect of heat treatment on UVB-induced wrinkle formation

We examined the effect of a single mild heat treatment (exposure to heated water, 42 °C for 5 minutes) on HSP expression in the dorsal skin of hairless mice. Immunoblotting analysis revealed that the level of HSP70 but not of other HSPs in the skin increased after the heat treatment (Figure 1a and b). The induction of expression of HSP70 by the mild heat treatment (42 °C for 5 minutes) was observed even after the repeated heat treatment (three times a week for 5 weeks) (Figure 1c and d). Costaining of HSP70 and pan-cytokeratin (a keratinocyte marker), vimentin (a fibroblast marker), or CD11b (a macrophage marker) was observed in both repeatedly heat-treated and untreated dorsal skin (Figure 1e–g). We confirmed mild heat treatment–induced expression of HSP70 in mice irradiated with UVB (Figure 1c–g).

To examine the effect of expression of HSPs on UVB-induced wrinkle formation, the dorsal skin of animals was pre-exposed to the heat treatment (exposure to heated water, 42 °C for 5 minutes) and then irradiated with UVB. This cycle was repeated three times a week for 10 weeks. As shown in Figure 2a and b, visible signs of wrinkling were observed in the dorsal skin of UVB-treated control mice (without heat treatment), but not so clearly in that of mice treated with both UVB and heat. The area of shadow on the replica images, which is indicative of wrinkle formation level, was increased by exposure to UVB radiation, whereas concomitant heat treatment reduced this index in UVB-treated mice (Figure 2c and d). These results suggest that the heat treatment suppresses UVB-induced wrinkle formation.

We then used a Cutometer to examine the effect of heat treatment on UVB-induced alterations to skin elasticity. All indexes of skin elasticity (Uf, final distension; Ue, immediate distension; and Ur, immediate retraction) except for Uv (delayed distension) were decreased by the UVB radiation and were significantly higher in heat-treated skin than in untreated skin exposed to UVB radiation (Figure 2e), suggesting that heat treatment suppresses the UVB-induced decrease in skin elasticity.

Epidermal hyperplasia is also closely linked to wrinkle formation. The UVB irradiation induced epidermal hyperplasia, although the epidermal thickness was lower in mice subjected to concomitant heat treatment than in control mice exposed to UVB radiation (Figure 2f and g).

We then used immunohistochemical analysis to examine the effect of the heat treatment on the ECM. As shown in Figure 3a, the layer expressing type IV collagen (the epidermal basal membrane) was disrupted in UVB-treated control mice (without heat treatment). This effect, however, was attenuated in mice concomitantly exposed to heat treatment.

Total expression of type I collagen and fine collagen fibers was decreased in UVB-exposed control mice (without heat treatment), and these decreases were suppressed in mice that had been concomitantly exposed to heat treatment (Figure 3a). Similar results were observed for elastic fibers, which were identified by the immunohistochemical detection of tropoelastin (Figure 3a). The results in Figure 3a suggest that heat treatment suppressed the UVB-induced disruption and degeneration of the skin's ECM.

UVB-induced wrinkle formation–related phenomena in transgenic mice expressing HSP70

We then compared the UVB-induced decrease in skin elasticity and epidermal hyperplasia between transgenic mice expressing HSP70 (Plumier *et al.*, 1995) and wild-type mice. UVB-induced decreased skin elasticity (decrease in Uf, Ue, and Ur indexes) was observed in wild-type mice; these indexes were significantly higher in UVB-treated transgenic mice expressing HSP70 (Figure 4a). Similar results were observed for epidermal hyperplasia; the epidermal thickness was lower in transgenic mice than in wild-type mice after UVB irradiation (Figure 4b and c). These results show that the UVB-induced decrease in skin elasticity and epidermal hyperplasia observed in wild-type mice was suppressed in transgenic mice expressing HSP70.

The UVB-induced degradation of the epidermal basal membrane and the decrease in collagen and elastic fibers were not observed as clearly in transgenic mice expressing HSP70 as they were in wild-type mice (Figure 3b).